BRAIN
ORIGINAL ARTICLE

Serotonergic dysfunction impairs locomotor coordination in spinal muscular atrophy

Nicolas Delestrée,[1,2] Evangelia Semizoglou,[1,2] John G. Pagiazitis,[1,2] Aleksandra Vukojicic,[1,2] Estelle Drobac,[1,3] Vasilissa Paushkin[1,2] and George Z. Mentis[1,2,3]

Neuromodulation by serotonin regulates the activity of neuronal networks responsible for a wide variety of essential behaviours. Serotonin (or 5-HT) typically activates metabotropic G protein-coupled receptors, which in turn initiate second messenger signalling cascades and induce short and long-lasting behavioural effects. Serotonin is intricately involved in the production of locomotor activity and gait control for different motor behaviours. Although dysfunction of serotonergic neurotransmission has been associated with mood disorders and spasticity after spinal cord injury, whether and to what extent such dysregulation is implicated in movement disorders has not been firmly established.

Here, we investigated whether serotonergic neuromodulation is affected in spinal muscular atrophy (SMA), a neurodegenerative disease caused by ubiquitous deficiency of the SMN protein. The hallmarks of SMA are death of spinal motor neurons, muscle atrophy and impaired motor control, both in human patients and mouse models of disease. We used a severe mouse model of SMA, that closely recapitulates the severe symptoms exhibited by type I SMA patients, the most common and most severe form of the disease. Together, with mouse genetics, optogenetics, physiology, morphology and behavioural analysis, we report severe dysfunction of serotonergic neurotransmission in the spinal cord of SMA mice, both at early and late stages of the disease. This dysfunction is followed by reduction of 5-HT synapses on vulnerable motor neurons.

We demonstrate that motor neurons innervating axial and trunk musculature are preferentially affected, suggesting a possible cause for the proximo-distal progression of disease, and raising the possibility that it may underlie scoliosis in SMA patients. We also demonstrate that the 5-HT dysfunction is caused by SMN deficiency in serotonergic neurons in the raphe nuclei of the brainstem. The behavioural significance of the dysfunction in serotonergic neuromodulation is underlined by inter-limb discoordination in SMA mice, which is ameliorated when selective restoration of SMN in 5-HT neurons is achieved by genetic means.

Our study uncovers an unexpected dysfunction of serotonergic neuromodulation in SMA and indicates that, if normal function is to be restored under disease conditions, 5-HT neuromodulation should be a key target for therapeutic approaches.

1 Center for Motor Neuron Biology and Disease, Columbia University, New York, NY 10032, USA
2 Department of Neurology, Columbia University, New York, NY 10032, USA
3 Department of Pathology and Cell Biology, Columbia University, New York, NY 10032, USA

Correspondence to: George Z. Mentis
Columbia University, P&S Building, Room 4-401
630 W 168th Street, New York, NY, 10032, USA
E-mail: gzmentis@columbia.edu

Keywords: motor neuron disease; SMA; serotonin; locomotion; synapse

Received April 25, 2022. Revised May 12, 2023. Accepted June 11, 2023. Advance access publication September 7, 2023

Introduction

Neuromodulation by serotonin, one of the two main monoamine neurotransmitters together with dopamine, has profound effects on brain function and behaviour. Given the widespread distribution of serotonergic synapses throughout the central and peripheral nervous systems, it is not surprising serotonin is implicated in various important biological functions such as movement, memory, anxiety, feeding, sleep, thermoregulation, neuroimmunomodulation as well as blood flow and glucose metabolism.[1–9] This neurotransmitter can modulate the synaptic properties, excitability and firing pattern of neural circuits and therefore alter their physiological output.[10] By altering neuronal properties, serotonin can select a particular functional output.[11,12] Additionally, previous studies have demonstrated that serotonin plays a role in axonal and dendritic remodelling, neuronal survival and neurogenesis during early stages of development,[13] and that impairment of early serotonin signalling leads to long lasting behavioural deficits.[5,14]

One of the fundamental functions of serotonin is the modulation of motor behaviours and motor control.[15] Humans and most mammals gain the ability to move over ground at early postnatal ages through the development and establishment of neural circuits within the spinal cord. These motor circuits are controlled by descending commands from brain regions and information received from the periphery.[16,17] Structures in the brainstem are responsible for initiation and speed regulation of locomotor behaviours.[18] The brainstem area that was originally proposed to initiate locomotion is known as the mesencephalic locomotor region (MLR).[19] Neurons within the MLR region communicate with reticulospinal neurons that ultimately connect directly with the spinal central pattern generator responsible for locomotor behaviour.[20] Within the brainstem, the two main neurotransmitter-identified neuronal groups suggested to be involved are glutamatergic and serotonergic.[21]

Experiments using *ex vivo* murine neonatal spinal cords have demonstrated that serotonin is involved in locomotor rhythmogenesis.[22–24] In addition, electrical or chemical stimulation of a parapyramidal region in the brainstem—which includes serotonergic neurons—produced coordinated locomotion, which was abolished following addition of 5-HT_{2A} and 5-HT_7 receptor antagonists.[25] Furthermore, mice lacking 5-HT_7 receptors can generate rhythmic activity, but with notable inter- and intra-limb disrupted coordination.[26] Finally, impairment of differentiation and maintenance of serotonergic neurons through *Pet1* knockout mice,[27] which lack 5-HT neurons exhibited locomotor defects.[28]

Changes in the spinal serotonergic innervation has been associated with spasticity after spinal cord injury[29] and reported to be affected in amyotrophic lateral sclerosis.[30] Gait, posture and locomotion, which are largely influenced by both proprioception and neuromodulation, are altered in patients with spinal muscular atrophy (SMA).[31–33] It is therefore possible that perturbations in serotonergic neurotransmission are playing a significant role in behavioural abnormalities observed in neurodegenerative diseases affecting the motor system. We sought to explore this fundamental question in the neurodegenerative disease SMA. SMA is caused by homozygous mutations in the ubiquitously expressed gene survival motor neuron 1 (*SMN1*),[34] causing SMN protein deficiency.[35,36]

The hallmarks of the disease are motor neuron death, muscle atrophy and impairment of motor function.[35–37] One of the earliest events arising during SMA is the dysfunction and elimination of proprioceptive sensory synapses on vulnerable motor neurons both in mouse models[38,39] and SMA patients.[40,41] This pathological event is mediated by several mechanisms including: aberrant activation of the classical complement pathway,[42] U12 splicing dysfunction[43] and stasimon (*TMEM41B*) dysfunction, a gene encoding an endoplasmic reticulum-resident transmembrane protein regulated by SMN.[44] Excitatory proprioceptive synapses that use VGluT1 are preferentially affected[38,39,45–49] in addition to VGluT2+ synapses from other excitatory pre-motor neurons,[46,50] which are also reduced, albeit to a smaller extent. Cholinergic synapses that contact motor neurons, including synapses from *Pitx2*$^+$ neurons[51] are also affected in SMA mouse models.[49] In contrast, inhibitory synapses—using GlyT2 and VGAT—appear to be unaffected throughout the course of disease.[38,46,49] However, it is unknown whether the neuromodulatory serotonergic system is affected in SMA.

To address this, we have used the severe SMN-Δ7 mouse model of SMA.[52] We used genetics, behavioural approaches combined with optogenetics, physiology, morphological assays together with confocal microscopy and image analysis. We report here that serotonergic neurotransmission is compromised early in disease onset and persists throughout the course of the disease in the SMN-Δ7 mouse model. 5-HT$^+$ synapses impinging on vulnerable motor neurons are dysfunctional and are subsequently lost in the course of the disease. The elimination of 5-HT synapses on motor neurons is governed by C1q, the initiating protein of the classical complement cascade. Importantly, the dysfunction and reduction of serotonergic synapses is caused by serotonergic-autonomous mechanisms as revealed by their rescue following selective genetic restoration of SMN in serotonergic neurons of SMA mice. The behavioural significance of serotonergic dysfunction in SMA mice is reflected by a severe inability in inter-limb coordination during locomotor behaviour. Our findings identify significant dysfunction in the neuromodulatory role of serotonergic-dependent neurotransmission, which must be corrected if effective therapies are to be adopted for the restoration of normal motor behaviour in SMA.

Materials and methods

Animals

All surgical procedures were performed on postnatal mice in accordance with the National Institutes of Health Guidelines on the Care and Use of Animals and approved by the Columbia animal care and use committee (IACUC). Animals of both sexes were used in this study. The original breeding pairs for the SMA mice used in our study (*Smn*$^{+/-}$; *SMN2*$^{+/+}$; *SMNΔ7*$^{+/+}$) were purchased from Jackson Mice (Jax stock #005025; FVB background) as well as Pet1^{CRE} (provided by Dr Rene Hen, Columbia University) and RosaChR2 [Ai32(RCL-ChR2(H134R)/EYFP]—(Jax stock # 012569). Pet1^{CRE} mice (C57Bl6 background) were bred to generate (*Pet1*$^{CRE+/-}$; *Smn*$^{+/-}$;*SMN2*$^{+/+}$;*SMNΔ7*$^{+/+}$) (referred to here as SMA::Pet1^{CRE}) mice. This strain was bred with SMA mice expressing a CRE-inducible *Smn* allele (*Smn*^{Res}; JAX stock #007951)[53]; CRE$^-$ SMA mice were null for the *Smn* allele, CRE-negative and carrying the *Smn*^{Res} allele (Pet1$^{CRE-/-}$;*Smn*$^{Res/-}$;*SMN2*$^{+/+}$;*SMNΔ7*$^{+/+}$). CRE$^+$ SMA animals were carrying one allele of the *Smn*^{Res}, absent of endogenous mouse *Smn* and heterozygous for *Pet1*^{CRE}, (*Pet1*$^{CRE+/-}$;*Smn*$^{Res/-}$;*SMN2*$^{+/+}$;*SMNΔ7*$^{+/+}$). Wild-type (WT) mice were homozygous for Smn in the absence of CRE (*Pet1*$^{CRE-/-}$;*Smn*$^{+/+}$;*SMN2*$^{+/+}$;*SMNΔ7*$^{+/+}$). The SMA::ChAT^{CRE} line was generated in a similar manner. SMA::Pet1+ChAT^{CRE} line was generated by crossing the two lines aforementioned. RosaChR2 mice were bred with Pet1^{CRE} mice to generate (*RosaChR2*$^{+/-}$; *Pet1*$^{CRE+/-}$) mice. In some tracing experiments we used ChAT^{CRE} (Jax stock # #006410) mice and crossed them with *lsl*-TdTomato mice (Jax stock # #007914).

Genotyping

Tail DNA PCR genotyping protocols for SMN-Δ7 mice were followed as described on the Jackson website. Customized primers used to genotype the *Smn*, Smn^{Res}, $Pet1^{CRE}$, $ChAT^{CRE}$ and *RosaChR2* alleles are listed in Supplementary Table 1. $Pet1^{CRE}$ and $ChAT^{CRE}$ primers allow discrimination between the two CRE+ alleles. A universal PCR reaction was used as follows: 12.5 µl of GoTaq Hot Start Green Master Mix (Promega), 0.5 µl of each primer (25 µM; Sigma), and 4 µl of 1:20 diluted lysed tail DNA in a final volume of 25 µl using dH_2O. For the *Smn* and Smn^{Res} alleles, products were amplified using the following thermal cycling method: 95°C for 2 min, followed by 35 cycles of 95°C for 1 min, 55°C for 1 min, 72°C for 1 min; and finally 72°C for 5 min. For the $Pet1^{CRE}$ allele: 95°C 3 min, 35 cycles of 95°C 1 min, 60°C 1 min 30 s, 72°C 1 min 30 s; then 72°C for 5 min. For the *RosaChR2* allele: 94°C 3 min, followed by 35 cycles of 94°C 20 s, 61°C 30 s and 72°C 30 s; then 72°C for 2 min.

Behavioural analysis

Mice from all experimental groups were monitored daily, weighed and the righting reflex was performed three times. Righting time was defined as the time for the pup to turn over after being placed completely on its back. The average time out of the three trials was calculated.[38] For the posture test, the animal was placed on its four limbs, and we measured the time for keeping the same posture. Posture time was defined as the time the pup maintained its balance prior to falling on its side after being placed on its four limbs. Three trials were averaged as described previously. The cut-off test time for the righting reflex and posture time was 60 s to comply with IACUC guidelines. Mice with a 25% daily weight loss and inability to right were euthanized with carbon dioxide to comply with IACUC guidelines for humane euthanasia.

Physiology using the intact *ex vivo* brainstem-spinal cord preparation

Methods used in this study to record motor neuron activity in the isolated *ex vivo* spinal cord have been in part described previously.[38,39,42] Animals were anaesthetized with an intraperitoneal injection of tribromoethanol (0.3 mg/g body weight) and decapitated at the level of the stereotaxic lambda in order to separate the forebrain from the rest of the CNS. The brainstem, cerebellum and spinal cord were dissected in continuity and removed from the carcass under cold (~12°C) artificial CSF (aCSF) containing in mM: 128.35 NaCl, 4 KCl, 0.58 $NaH_2PO_4.H_2O$, 21 $NaHCO_3$, 30 D-glucose, 1.5 $CaCl_2.H_2O$, and 1 $MgSO_4.7H_2O$. The cerebellum was then separated from the brainstem and the brainstem-spinal cord group was transferred (ventral side up) to a customized recording chamber perfused continuously with oxygenated (95% O_2/5% CO_2) aCSF (~10 ml/min) at room temperature. Dorsal and ventral roots from the first and fifth lumbar segments were placed into suction electrodes for stimulation or recording, respectively. Dorsal roots stimulation: 20–100 µA, 0.2 ms pulses. A custom-made bipolar concentric electrode was inserted superficially in the pons for raphe nuclei stimulation, controlled by TTL pulses (using Clampex software) using an A365 stimulus isolator. Brainstem conditioning stimulation: 5 s train of 100–300 µA (supramaximal stimulation intensity, above the intensity necessary to reach the maximal spinal reflex conditioning effect), 0.2 ms pulses at 5 Hz. In some experiments, a cocktail of serotonergic receptors inhibitors [WAY100635 (5-$HT1_A$ receptor antagonist) (10 µM); ketanserin (5-HT2/6 receptor antagonist) (10 µM); SB206653 (5-$HT2_C$ receptor antagonist) (10 µM); SB269970 (5-HT7 receptor antagonist) (10 µM)] was perfused in the bath. In the case of drug application, data collection started 20 min after drug application. Following washout of drugs, data were collected after 20–30 min after washout initiation. Electrical stimulations were delivered using an A365 stimulus isolator controlled by the Clampex10 software (Molecular Devices). Recordings were made using an SW-10 preamplifier (CWE) and a proAmp-8 programmable amplifier (CWE) connected to a Digidata1440A interface and using the Clampex software. Sampling rate: 50 kHz. In experiments involving mice expressing ChR2 in brainstem serotonergic cells, we used a TTL-pulse controlled pE-100 (CoolLED) 470 nm light source directed to the brainstem to deliver optical stimulation through a ⌀2 mm fibre optic delivering 50 mW at the tip. Brainstem optical conditioning stimulation: 5 s train of 100 ms pulses at 5 Hz. After the recording session, the brainstem and spinal cord were fixed in 4% paraformaldehyde (PFA) overnight and subsequently transferred to 0.01 M phosphate-buffered saline (PBS) and processed for immunohistochemistry, as described below and in Supplementary Table 2.

Recordings during *in vivo* locomotor activity

Ten day old mice (P10) were anaesthetized with isoflurane (5% induction, 2–3% maintenance) and the skin of each hindlimb (for tibialis anterior) or groin (for psoas) was incised bilaterally. A pair of thin (0.003″ bare; 0.0055″ coated; A-M Systmes) Teflon-coated silver wire electrodes were inserted 0.5 mm deep and sutured in the belly of each tibialis anterior or psoas muscle (2–3 mm between each electrode). The skin was then closed and sutured around the electrode cables. Following 30 min recovery, the electrodes were connected to an amplifier and the EMG activity of each side of the tibialis anterior or psoas muscles was collected simultaneously for 1 h during voluntary locomotion. SMA animals were assisted to keep a standing posture allowing locomotion. After the recording session, the mice were anaesthetized with a tribromoethanol (0.3 mg/g) intra-peritoneal injection and transcardially perfused with PBS followed by 4% PFA. The brainstem and spinal cord were then isolated, fixed in 4% PFA overnight and subsequently transferred to 0.01 M PBS and processed for immunohistochemistry as described below and in Supplementary Table 2.

Somatodendritic labelling of motor neurons

Experimental protocols used in this study have been previously described.[38] Four day old (P4) and P10 mice were used in tracing and immunohistochemistry experiments. Following isolation of the spinal cord from the vertebral column (as described above), the spinal cord was transferred to a dissection chamber and the L1 and L5 ventral roots were placed inside suction electrodes and backfilled with a fluorescent dextran to label the motor neurons from the cut end of the ventral root (Supplementary Table 2). The intact cord was perfused with cold (~10°C), oxygenated (95% O_2/5% CO_2) aCSF (containing in mM: 128.35 NaCl, 4 KCl, 0.58 $NaH_2PO_4.H_2O$, 21 $NaHCO_3$, 30 D-glucose, 0.1 $CaCl_2.H_2O$, and 2 $MgSO_4.7H_2O$). After 12–24 h the cord was immersion-fixed in 4% PFA solution for 24 h and washed in 0.01 M PBS. Spinal cord sections were subsequently processed for immunohistochemistry as described below with antibodies shown in Supplementary Table 2.

CTb tracing

To reveal the localization of brainstem neurons innervating the spinal cord and the spinal motor neurons innervating the

multifidus muscle, Cholera Toxin subunit B (CTb) was injected into the lumbar spinal cord at P0 or in the multifidus muscle at P2, respectively. The animals were anaesthetized with isoflurane, a small incision was performed in the skin and ~0.5 µl were injected in the muscle or in the spinal cord through the intervertebral space. The animals were put back with the rest of the litter until P4, when they were perfused with 4% PFA and the tissues sampled. The sites of injection were also checked to verify that no spillover to other tissues occurred.

Immunohistochemistry

Immunohistochemical protocols used in this study have been described previously.[38,42] Details of fixatives and immunohistochemical protocols used in this study are included in Supplementary Table 2. All antibodies, except those targeted parvalbumin and VGluT1, are commercially available (Supplementary Table 2). Chicken anti-parvalbumin was produced by Covance and designed against a full-length bacterial fusion protein; Guinea pig anti-VGluT1 antibody was also produced by Covance and designed against the epitope (C)GATHSTVQPPRPPPP, which lies within the N-terminus of mouse VGluT1. The VGluT1 antibody was validated in VGluT1 knockout tissue.[39] The tissue was embedded in warm 5% agar and serial sections were cut on a vibratome (75–100 µm thickness). Sections were blocked with 10% normal donkey serum in 0.01 M PBS with 0.1% Triton X-100 (PBS-T; pH 7.4) and incubated overnight at room temperature in different combinations of antisera in PBS-T (Supplementary Table 2). For experiments involving mouse-raised primary antibodies, sections were preincubated for 1 h in 'mouse on mouse' (M.o.M) blocker (Vector Laboratories) in PBS-T to block endogenous antigens. The following day, sections were washed in PBS-T and secondary antibody incubations were performed for 3 h with the appropriate species-specific antiserum diluted in PBS-T. Sections were subsequently washed in PBS, mounted on glass slides using Fluoromount-G (Invitrogen). In the case of the usage of two primary antibodies raised in the same host species, we ran the protocol sequentially for each of them. Between each protocol, we incubated the sections in 10% host serum in PBS-T for 3 h followed by an overnight incubation in a solution of unconjugated antigen-binding fragment (Fab) targeted to the host at 50 µg/ml of PBS-T (Supplementary Table 2).

Imaging and analysis

Sections were scanned using an SP8 Leica confocal microscope and analysed using ImageJ and Neurolucida (MBF Bioscience). For all immunohistochemical analysis, at least three animals were used for each genotype. At least 30 brainstem serotonergic neurons were included from each animal for each genotype. To quantity the proportion of serotonergic-positive brainstem cells expressing ChR2 and the specificity of the ChR2 expression to serotonergic neurons, we enhanced EYFP ChR2-reporter expression with anti-GFP antibodies and counted the number of 5-HT-positive cells expressing EYFP and the number of EYFP-positive cells expressing 5-HT, respectively. In the first 200 µm ventral part of the brainstem z-stack single plane optical images (0.09 µm/px; 1.038 µm optical section; 0.35 µm z-steps) were acquired with a 40× objective.

For SMN quantification, the number of brainstem serotonergic neurons or proprioceptive (parvalbumin+) neurons with either present or absent nuclear SMN gems was counted from z-stack single optical plane scans (0.09 µm/px; 1.038 µm optical section; 0.35 µm z-steps), acquired with a 40× objective. At least 20 brainstem serotonergic neurons and proprioceptive neurons were included from each animal for each genotype. For brainstem serotonergic cells count, we analysed the most superficial 300 µm ventral brainstem sections containing the nucleus raphe pallidus[54] using a 20× objective. Only 5-HT+ neurons that contained the nucleus were counted in order to avoid double counting the same neuron present in adjoining sections. For motor neuron counts, we analysed 12 z-stack (0.14 µm/px; 2.055 µm optical section; 0.68 µm z-steps) images collected from the entire L1 segment (12 sections) using a 20× objective. Only motor neurons (ChAT+) that contained the nucleus were counted to avoid double counting.

Quantitative analysis of VGluT1 and 5-HT immunoreactive synaptic densities on motor neurons at P4 and P10 was performed on z-stack (0.09 µm/px; 1.038 µm optical section; 0.35 µm z-steps) images acquired using a 40× objective and including the whole cell body and dendrites of retrogradely labelled motor neurons. To obtain synaptic densities on somata and dendrites, we reconstructed 3D models of the labelled motor neurons using Neurolucida and we marked the VGluT1 and 5-HT contacts. We then calculated the somatic densities as the total number of synapses for the entire soma and the dendritic densities, as the number of synapses per 50 µm centripetal compartments (0–50, 50–100 and 100–150 µm) starting from the soma and following the dendrites trajectory, using a custom-made Visual Basic macro. Only neurons with the entire soma included within the z-stack were considered for analysis. Analysis of C1q deposition on 5-HT synapses was performed on z-stack (0.06 µm/px; 1.038 µm optical section; 0.35 µm z-steps) images acquired using a 40× objective. Only synapses contacting motor neurons on soma were included in the analysis. Synapse was determined as 'tagged' if C1q signal co-localized with the presynaptic signal, which was confirmed using the intensity line profiling tool, where synaptic markers and C1q intensity line profiles overlapped. We counted all synaptic contacts on the entire soma against the tagged synapses on soma, respectively, to obtain the percentage of tagged synapses.

Statistics

Results are expressed as means ± standard error of the mean (SEM) unless otherwise specified. The number of animals is reported as 'N' and the sample size as '*n*' for each dataset. Statistical analysis was performed using GraphPad Prism 6. The d'Agostino and Pearson omnibus normality test (or Shapiro-Wilk normality test for samples size <8) was used to assess the normality for all data. Comparisons were performed by either Student's *t*-test or one-way ANOVA (*post hoc* comparison methods are indicated in the 'Results' sections and figure legends, when necessary) for normally distributed datasets, non-parametric Mann-Whitney-Wilcoxon and Kruskal-Wallis tests were used otherwise.

To study the spatial distribution of VgluT1 synapses in relation to 5-HT synapses location in the dendritic tree, we computed the nearest neighbour index (Rn) using the following formula:

$$Rn = D(Obs)/\ 0.5(1/n - 1) \quad (1)$$

where D = observed mean of nearest serotonergic synapse distance; l = dendritic length considered; and n = number of serotonergic synapses.

For circular datasets, von Mises distribution was assessed using Watson's test. Rayleigh test was used to confirm a preferential angular direction for each dataset. Wallraff test was used to compare several groups to each other.

Finally, Gehan-Breslow-Wilcoxon test was used to compare survival curves.

A statistical significance was considered at $^{*}P < 0.05$, $^{**}P < 0.01$, $^{***}P < 0.001$ and $^{****}P < 0.0001$.

No statistical methods were used to predetermine sample sizes but our sample sizes were similar to those reported in previous publications.[38,55,56] No randomization was used. Data collection was not performed blind to the conditions of the experiments, however, analysis was performed blind.

Results

Serotonergic transmission inhibits the monosynaptic dorsal-to-ventral root response

Serotonin or 5-HT, is a monoamine neurotransmitter acting on 5-HT receptors located on spinal motor neurons,[57,58] spinal interneurons[59–61] and primary afferent sensory fibres.[62] To test the function of 5-HT neurotransmission in neonatal mice, we took advantage of previous reports demonstrating the 5-HT effect on inhibiting the dorsal-to-ventral root monosynaptic response in neonatal rodents.[63–66] We used this neuromodulatory effect as a proxy to study serotonergic function in the spinal motor circuits.

We used the *ex vivo* brainstem-spinal cord preparations from neonatal mice and focused on the first (L1) and fifth lumbar (L5) segments, because SMA motor neurons are differentially affected in these spinal segments, with L1 being the most vulnerable. To identify 5-HT neurons innervating the spinal cord early after birth, the tracer CTb-555 (CTb coupled with Alexa 555 dye) was injected *in vivo* at P0 in the lumbar spinal region. At P4, brainstem examination revealed that nearly all neurons in the raphe pallidus and some in the raphe obscurus were 5-HT^{+} and CTb-555^{+} (Fig. 1A and B), identifying this brainstem region as a source of 5-HT.

First, we induced the monosynaptic reflex amplitude recorded in the ventral root following stimulation of the homonymous dorsal root in wild-type animals. We then measured and compared the amplitude of the monosynaptic response in L1 and L5 segments prior to and after a conditioning electrical stimulation of the ventral raphe nuclei in the brainstem (Fig. 1C). The ventral raphe nuclei were stimulated for 5 s at 5 Hz at supramaximal intensity (1.5× the intensity that produced the maximal conditioning effect). The unconditioned and conditioned successive dorsal-to-ventral root responses were separated by 60 s (Fig. 1C) to ensure maximum recovery of the monosynaptic reflex amplitude in absence of the brainstem stimulation.[39,67] We found that this conditioning stimulation protocol resulted in ∼50% reduction of the monosynaptic reflex response in P4 wild-type mice (Fig. 1D and E). To test whether the reduction of the monosynaptic reflex was due to serotonergic release, we applied the following major 5-HT receptor blockers, WAY100635 (5-HT$_{1A}$ receptor antagonist, 10 µM), ketanserin (5-HT$_{2/6}$ receptor antagonist, 10 µM), SB206653 (5-HT$_{2C}$ receptor antagonist, 10 µM) and SB269970 (5-HT$_{7}$ receptor antagonist, 10 µM). We found that, following ∼20 min of bath application of the blockers, there was a substantial reversal of the reduction of the monosynaptic reflex (Fig. 1D and E), which was partially recovered upon washout (Fig. 1D and E). These results demonstrate that the reduction of the monosynaptic response following electrical stimulation of the ventral raphe nuclei of the brainstem was largely due to serotonergic release.

Electrical stimulation of the ventral brainstem in the *ex vivo* brainstem-spinal cord preparation may result in inappropriate stimulation of neurons beyond the raphe nuclei. To address this possibility, we used an optogenetic approach to selectively activate 5-HT neurons in the ventral raphe nuclei. We used mice generated from floxed ChannelRhodopsin 2-GFP (*lsl*-ChR2-GFP) crossed with Pet1^{CRE} mice. Pet1^{CRE} mice express Cre-recombinase exclusively in *Pet1*$^{+}$ expressing neurons, enabling Cre-dependent targeting to 5-HT neurons.[27,68] The efficacy of this mouse cross resulted in ∼66% of 5-HT neurons expressing ChR2, as visualized by the GFP reporter (Supplementary Fig. 1A and B). We then used the *ex vivo* brainstem-spinal cord preparation from Pet1^{CRE}-ChR2 mice to photoactivate 5-HT neurons bilaterally in the ventral raphe nuclei at P10 with 470 nm light delivered through a LED. The monosynaptic dorsal-to-ventral root reflex was conditioned by photoactivation of 5-HT neurons for 5 s—similar to the conditioned protocol during electrical stimulation of the ventral raphe of the brainstem. We found that the conditioned reflex by photoactivation resulted in ∼67% reduction of the reflex (Supplementary Fig. 1C and D). Importantly, we subsequently performed electrical stimulation in the same spinal cords (similar to the experiments in Fig. 1A and D) and found that electrical conditioning of the monosynaptic reflex resulted in ∼74% reduction of the reflex (Supplementary Fig. 1C and D). These experiments demonstrate that the reduction of the monosynaptic dorsal-to-ventral response is due to activation of 5-HT neurons in ventral raphe nuclei.

Serotonergic neurotransmission is impaired in a mouse model of SMA

To investigate the function of serotonergic neurotransmission in the neurodegenerative disease SMA, we used the severe SMN-Δ7 mouse model.[52] Having validated our conditioned protocol of the monosynaptic spinal reflex by electrical stimulation, we performed the same type of experiments in SMA mice and controls in L1 and L5 segments at early (P4) and late (P10) stages of disease. The L1 segment contains vulnerable motor neurons innervating proximal muscles (i.e. iliopsoas, quadratus lumborum), while the L5 segment is dominated by a large resistant population of lateral motor column (LMC) motor neurons (∼94%, 700 L5-LMC out of 745 L5 motor neurons[38]) in comparison to the smaller but vulnerable medial motor column (MMC) motor neuron pool (∼6%, 45 L5-MMC out of 745 L5 motor neurons[38]) (Fig. 1C). At P4, the ∼40% reduction of the monosynaptic reflex observed in wild-type animals after conditioning by electrical stimulation of the ventral raphe nuclei was nearly absent (∼8%) in SMA mice in the L1 segment, indicating a significant impairment in serotonergic transmission in SMA mice (Fig. 1F and G). In contrast, there was no significant difference in the L5 segment following brainstem conditioning, in agreement that the L5 segment is largely a resistant spinal segment, not affected in SMA (Fig. 1F and G). Experiments performed at P10 revealed similar results to those at P4, indicating that serotonergic neurotransmission is severely compromised in the vulnerable L1 segment (Fig. 1H and I). Taken together, these results demonstrate that the serotonergic system is selectively affected by SMN deficiency during early stages and persists throughout the disease course.

Selective loss of serotonergic synapses from vulnerable motor neurons in SMA mice

Given the impairment of serotonergic neurotransmission in vulnerable spinal segments, we investigated whether there is a selective reduction in 5-HT synapses in SMA mice. To do so, we visualized the somato-dendritic morphology of spinal motor neurons by retrograde fill with fluorescent dyes using the *ex vivo* spinal cord (Fig. 2A). We

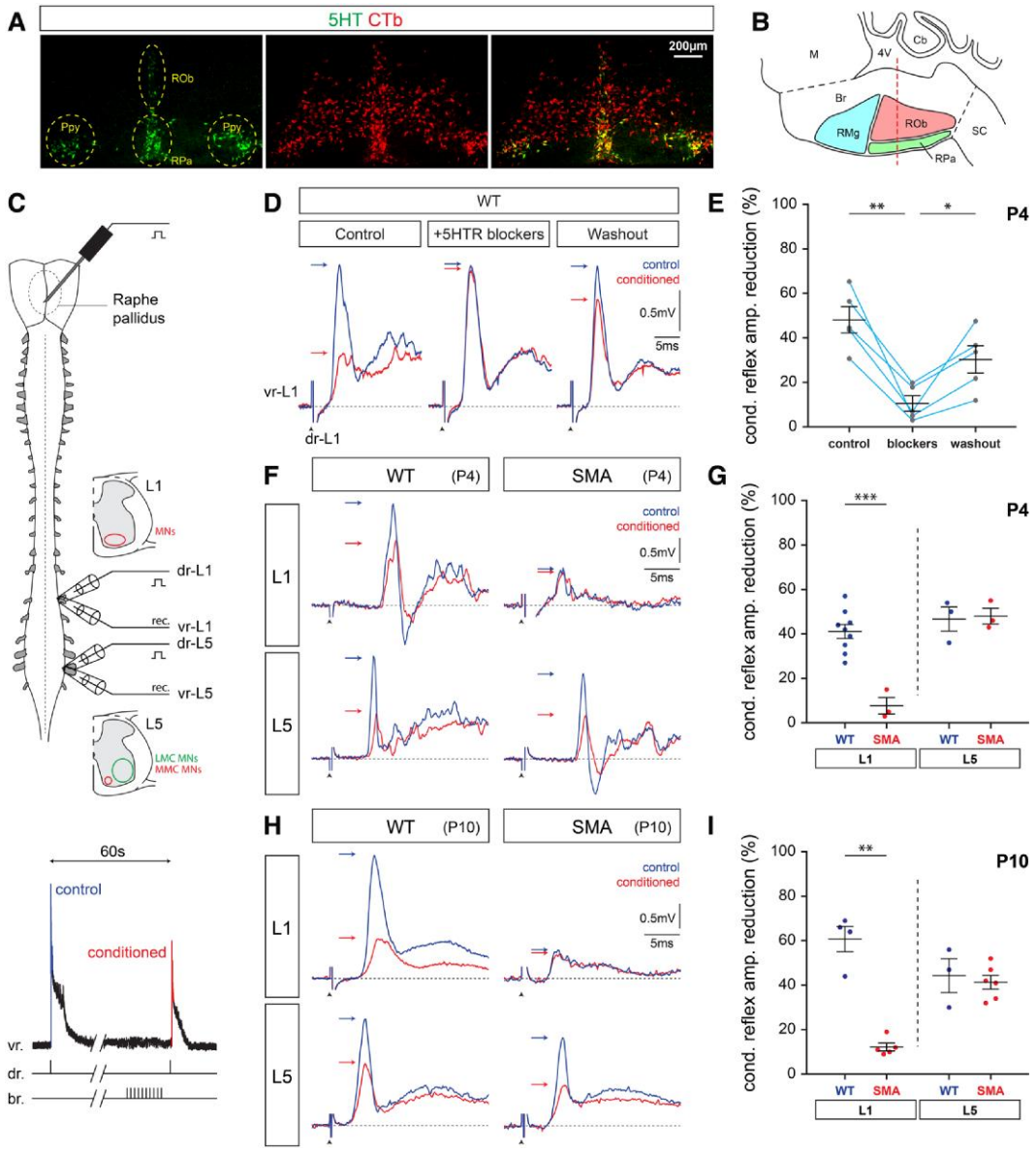

Figure 1 Serotonergic dysfunction is evident at the onset of SMA. (**A**) Single optical plane confocal images from transverse sections of the brainstem at P4 showing 5-HT immunoreactivity (in green) and CTb-555 (in red) injected in the lumbar spinal cord at P0/1 ($n = 3$ mice). (**B**) Drawing of the brainstem with the three main ventral raphe nuclei. Red dotted line is the approximate point of the transverse section shown in **A**. RPa = raphe pallidus; ROb = raphe obscurus; RMg = raphe magnus; M = midbrain; 4V = 4th ventricle; Cb = cerebellum; SC = spinal cord. (**C**) Illustration of the experimental set-up (*top*) for monosynaptic spinal reflexes and brainstem electrical stimulation used to study the modulatory effect of serotonin on the spinal reflex in L1 and L5 spinal segments. The hemicord schematics show the location and relative size of the motor neurons pools found in both lumbar segments. MNs = motor neurons; LMC = lateral motor column; MMC = medial motor column. Conditioning stimulation protocol of the dorsal-to-ventral root reflex (*bottom*). Ventral root (vr) responses following dorsal root (dr) stimulation are depicted in blue prior to brainstem (br) conditioning stimulation and in red, shortly after brainstem stimulation. The period before and after conditioning was 60 s. (**D**) Monosynaptic responses (horizontal arrows indicate maximum amplitude) in the L1 spinal segment before (in blue) and after (in red) brainstem conditioning stimulation in P4 wild-type (WT) mouse. Three conditions are shown as: control solution (*left*), during 5-HT receptor blockers (combined: WAY100635, ketanserin, SB206553 and SB269970) application (*middle*) and after washout (*right*). Horizontal arrows indicate maximum amplitude of monosynaptic response during control (blue arrows) and after conditioning (red arrows). Arrowhead = stimulus artefact. (**E**) Quantification of the effect of brainstem stimulation on the L1 monosynaptic reflex amplitude (expressed as percentage reduction) under the three conditions in (**D**). Measurements from the same experiment are linked with blue lines. Repeated measures ANOVA with Greenhouse-Geisser correction, Tukey's *post hoc* test. Control versus blockers $^{**}P = 0.0076$; blockers versus washout $^{*}P = 0.0459$; $n = 5$ mice. (**F**) Monosynaptic responses elicited in L1 and L5 spinal segments in P4 wild-type and SMA mice, before (blue) and after (red) brainstem conditioning stimulation. (**G**) Quantification of the conditioning effect of serotonin (percentage of reduction) in the monosynaptic reflex at P4. WT: L1, $n = 8$, SMA: L1, $n = 3$; *t*-test with Welch's correction. $^{***}P = 0.0009$. WT: L5, $n = 3$, SMA: L5, $n = 3$; *t*-test with Welch's correction. $P = 0.8499$. (**H**) Monosynaptic responses obtained in P10 wild-type and SMA mice. (**I**) Quantification of the conditioning effect of serotonin in the monosynaptic reflex at P10. WT: L1, $n = 4$; SMA: L1, $n = 5$; *t*-test with Welch's correction. $^{**}P = 0.0019$. WT: L5, $n = 3$, SMA: L5, $n = 6$; *t*-test with Welch's correction. $P = 0.7422$. SMA = spinal muscular atrophy.

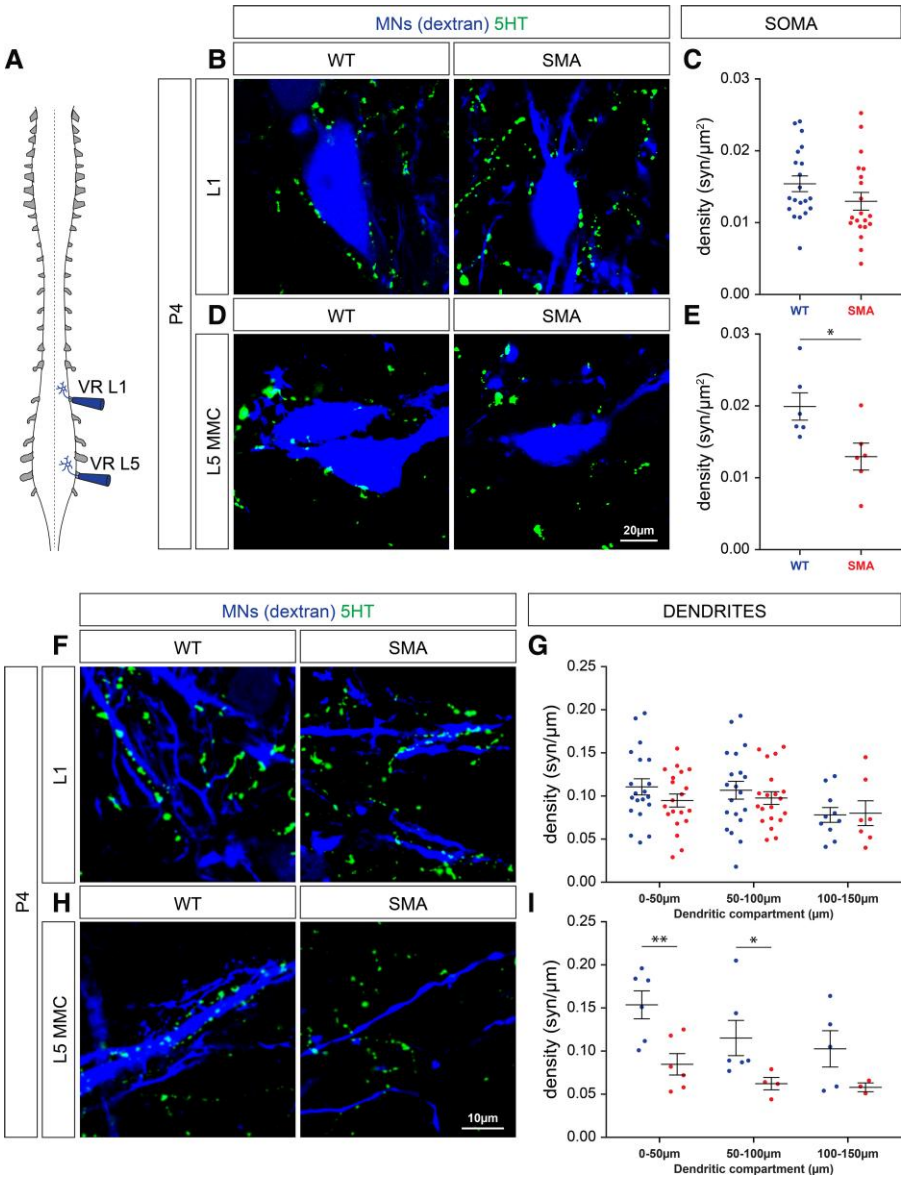

Figure 2 Loss of serotonergic synapses on motor neurons in SMA. (**A**) Illustration of the experimental protocol used for the retrograde labelling of L1 and L5 motor neurons. Suction electrodes were placed in the ventral roots L1 (VR-L1) and L5 (VR-L5). (**B**) Z-stack projections (total: 5 µm) of confocal single optical plane images showing retrogradely filled motor neurons (blue) and 5-HT immunoreactivity (green) in wild-type (WT) and spinal muscular atrophy (SMA) mice at P4. (**C**) Quantification of the somatic 5-HT synaptic surface density in L1 wild-type and SMA motor neurons. WT: $N = 4$, $n = 20$; SMA: $N = 4$, $n = 20$; *t*-test with Welch's correction. $P = 0.1482$. (**D**) As in **B**, showing L5 medial motor column (MMC) wild-type and SMA motor neurons. (**E**) As in **C** for L5 MMC wild-type and SMA motor neurons. WT: $N = 4$, $n = 6$; SMA: $N = 4$, $n = 6$; *t*-test with Welch's correction. $^{*}P = 0.0259$. (**F**) Z-stack projections (total: 2.75 µm) of confocal images of motor neuron dendrites (blue) and 5-HT immunoreactivity (green) from wild-type and SMA mice at P4. (**G**) Quantification of 5-HT synaptic densities in different dendritic compartments (0–50, 50–100 and 100–150 µm from the soma) from L1 wild-type and SMA motor neurons. 0–50 µm: WT, $N = 4$, $n = 20$; SMA, $N = 4$, $n = 20$; *t*-test with Welch's correction. $P = 0.1973$. 50–100 µm: WT, $N = 4$, $n = 20$; SMA, $N = 4$, $n = 20$; *t*-test with Welch's correction. $P = 0.4803$. 100–150 µm: WT, $N = 4$, $n = 10$; SMA, $N = 4$, $n = 7$; *t*-test with Welch's correction. $P = 0.9074$. (**H**) As in **F**, for L5 MMC motor neuron dendrites. (**I**) As in **G**, for L5 MMC motor neurons. 0–50 µm: WT, $N = 4$, $n = 6$; SMA, $N = 4$, $n = 6$; *t*-test with Welch's correction. $^{**}P = 0.0081$. 50–100 µm: WT, $N = 4$, $n = 6$; SMA, $N = 4$, $n = 4$; *t*-test with Welch's correction. $^{*}P = 0.0492$. 100–150 µm: WT, $N = 4$, $n = 5$; SMA, $N = 4$, $n = 3$; *t*-test with Welch's correction. $P = 0.1110$. N = number of mice; n = number of motor neurons; MNs = motor neurons.

then used immunohistochemistry against 5-HT (Supplementary Fig. 2A), confocal microscopy and image analysis using Neurolucida to quantify the somatic (surface density) and dendritic coverage (longitudinal synaptic density) in the proximal dendritic compartments (0–50, 50–100 and 100–150 µm from the soma) by 5-HT synapses. We performed our studies in L1 and L5 motor neurons in wild-type and SMA mice at P4, an age at which the deafferentation of proprioceptive synapses is already evident.[38]

We found that 5-HT synaptic coverage on the somata of L5 MMC, but not L1 motor neurons, was significantly lower in SMA mice compared to wild-type controls (Fig. 2B–E). A similar significant reduction was observed for the proximal dendritic compartments in the L5 MMC motor neurons in SMA (Fig. 2H and I), but not in dendrites of L1 motor neurons (Fig. 2F and G). Serotonergic coverage in the L5 LMC did not exhibit any significant difference between wild-type and SMA mice either on their somata (Supplementary

Fig. 2C and D) or dendrites (Supplementary Fig. 2E and F). The results from the L1 motor neurons demonstrate that the reduction of serotonergic transmission is due to synaptic dysfunction rather than the loss of 5-HT synapses. In the L5 spinal segment, although there was no significant functional dysfunction, the synaptic loss in the L5 MMC motor neurons only, is masked (absence of effect on the monosynaptic response by conditioning of the brainstem) by the higher number of L5 LMC motor neurons, which are not affected. The small number of MMC motor neurons innervate axial muscles such as multifidus, as demonstrated by retrogradely labelling by CTb-647 injected in the multifidus muscle (Supplementary Fig. 2B; $n = 4$ mice). In contrast, LMC motor neurons (which account for ~94% of L5 motor neurons) innervate hindlimb muscles (gastrocnemius and soleus muscles). Taken together, these results demonstrate that motor neurons innervating axial musculature are affected to a greater extent, followed by motor neurons innervating proximal muscles, while motor neurons innervating distal muscles are not affected by serotonergic dysfunction. These observations may explain the proximo-distal progression of disease in SMA.

Selective restoration of SMN in 5-HT neurons improves serotonergic neuromodulation in SMA mice

To test the origin of the impairment of serotonergic transmission, we genetically restored SMN in serotonergic neurons only. To do so, we used a mouse model of SMA harbouring a single targeted mutation and two transgenic alleles, resulting in the genotype $Smn^{Res/+}$;$SMN2^{+/+}$;$SMN\Delta7^{+/+}$ (where *Smn* is used for the mouse *Smn1* gene and *SMN* for the human *SMN2* gene).[53] The allele carrying the targeted mutation (Smn^{Res}) is engineered to revert to a fully functional *Smn* allele upon Cre-mediated recombination ($Cre^{+/-}$; $Smn^{Res/-}$;$SMN2^{+/+}$;$SMN\Delta7^{+/+}$).[53] *SMN2* is the human gene and SMNΔ7 corresponds to the human SMN cDNA lacking exon 7. In the absence of the Cre recombinase ($Cre^{-/-}$;$Smn^{Res/-}$;$SMN2^{+/+}$; $SMN\Delta7^{+/+}$) the phenotype of these mice is similar to that of the SMNΔ7 SMA mice.[53] This approach has been previously validated.[39,56,69,70] Restoration of SMN protein in 5-HT neurons was achieved by crossing the conditional inversion SMA mice with $Pet1^{CRE}$ mice, which express CRE under the control of the *Pet1* promoter (Fig. 3A) in 5-HT neurons.[27,68]

To examine the efficacy and specificity of SMN upregulation following CRE recombination in 5-HT neurons, we used SMN immunohistochemistry to study the presence of gems, nuclear structures containing SMN,[71] in 5-HT neurons in the raphe pallidus nucleus at P10 (Fig. 3B and C). We found that 95% of wild-type 5-HT neurons expressed gems, compared to none in SMA and ~50% in SMA::$Pet1^{CRE}$ mice (Fig. 3C). The CRE-recombination efficacy and restoration of SMN in 5-HT neurons was similar to our previously published observations for proprioceptive neurons and motor neurons.[39] Importantly, Pet1-CRE recombination was selective in 5-HT neurons, since we did not observe any gems in proprioceptive neurons, which are parvalbumin+ in dorsal root ganglia of SMA::$Pet1^{CRE}$ mice (Supplementary Fig. 3A and B). Collectively, these results confirm selective SMN restoration in a large fraction of 5-HT neurons.

We first sought to address whether 5-HT neurons degenerate in SMA. We counted the number of 5-HT neurons in the raphe pallidus nucleus and found no differences between the groups (Fig. 3D and E). We then investigated the effects of selective SMN restoration in 5-HT neurons on the reduced neuromodulatory effect of serotonin on the monosynaptic spinal reflex in SMA at P10. SMN restoration in 5-HT neurons of SMA mice (SMA::$Pet1^{CRE}$) significantly improved the serotonin-dependent reduction of the monosynaptic reflex in the L1 spinal segment following conditioning stimulation of the ventral raphe nuclei (Fig. 3F and G). As expected, there was no significant difference in the resistant L5 spinal segment (Fig. 3F and G). Importantly, the amplitude of the monosynaptic dorsal-to-ventral reflex response was not improved in the L1 spinal segment in SMA::$Pet1^{CRE}$ mice (Supplementary Fig. 3C and D). These results identify SMN deficiency in 5-HT neurons as the cause of the serotonergic dysfunction and 5-HT synaptic loss in SMA mice.

Loss of 5-HT synapses in SMA is caused by serotonergic-autonomous mechanisms

To investigate whether the loss of serotonergic synapses in SMA mice is due to motor neuron-autonomous or serotonergic-autonomous mechanisms, we performed a detailed analysis of synaptic coverage by 5-HT^{+} synapses on both somata and dendritic compartments in SMA::$Pet1^{CRE}$, SMA::$ChAT^{CRE}$ (selective SMN restoration in motor neurons), SMA and wild-type motor neurons. To reveal the largest possible extent of dendritic morphology, we labelled spinal motor neurons by retrograde fill using the *ex vivo* spinal cord preparation and performed immunohistochemistry against 5-HT. Z-stacks acquired by confocal microscopy and 3D reconstruction of the neurons revealed that the total number of 5-HT synapses covering the entire soma of L1 and L5 MMC vulnerable motor neurons were significantly reduced in SMA mice compared to wild-type mice (Fig. 4A–D). Selective restoration of SMN in 5-HT neurons (SMA::$Pet1^{CRE}$ mice) revealed a significant increase in 5-HT synapses compared to SMA mice, whereas restoration of SMN in motor neurons (SMN::$ChAT^{CRE}$ mice) did not (Fig. 4A–D). Similar results were observed for the proximal dendrites of the L5 MMC motor neurons (Fig. 4E–H), but the dendritic 5-HT synaptic coverage of L1 motor neurons did not reveal any significant changes in any of the experimental groups (Fig. 4E and F). A possible explanation for this observation is that the synaptic coverage of motor neuron dendrites by 5-HT synapses is higher in L5 MMC motor neurons compared to L1 motor neurons in wild-type mice (Fig. 4E–H) and therefore easier to detect changes in synaptic loss or due to the difference in the developmental time course of 5-HT+ synaptic coverage. In support of this possibility, in wild-type animals between P4 and P10, the number of 5-HT synapses increases by a 3-fold factor in L1 somata, while in L5-MMC the increase was only 1.5-fold. Alternatively, L1 motor neurons might exhibit loss of 5-HT synapses from their dendrites in later stages compared to the loss of 5-HT synapses from their soma. Unlike L5 MMC motor neurons, L5 LMC motor neurons did not reveal any significant differences in 5-HT synaptic coverage either on the motor neuron somata or on their proximal dendrites (Supplementary Fig. 4A–D). Taken together, these results indicate that there is a selective 5-HT synaptic loss in the vulnerable L5 MMC motor neurons (in both somatic and dendritic coverage), whereas L1 motor neurons exhibit a less severe synaptic reduction around their somata, but not on their dendrites. As expected from our previous work, L5 LMC motor neurons, considered resistant in SMA, did not reveal any overt synaptic changes in serotonergic synapses. Importantly, the 5-HT synaptic loss is due to SMN deficiency in serotonergic neurons, without post-synaptic effects from SMN-deficient motor neurons. These results indicate that 5-HT synaptic loss occurs in a manner consistent with the proximo-distal progression of disease in SMA.

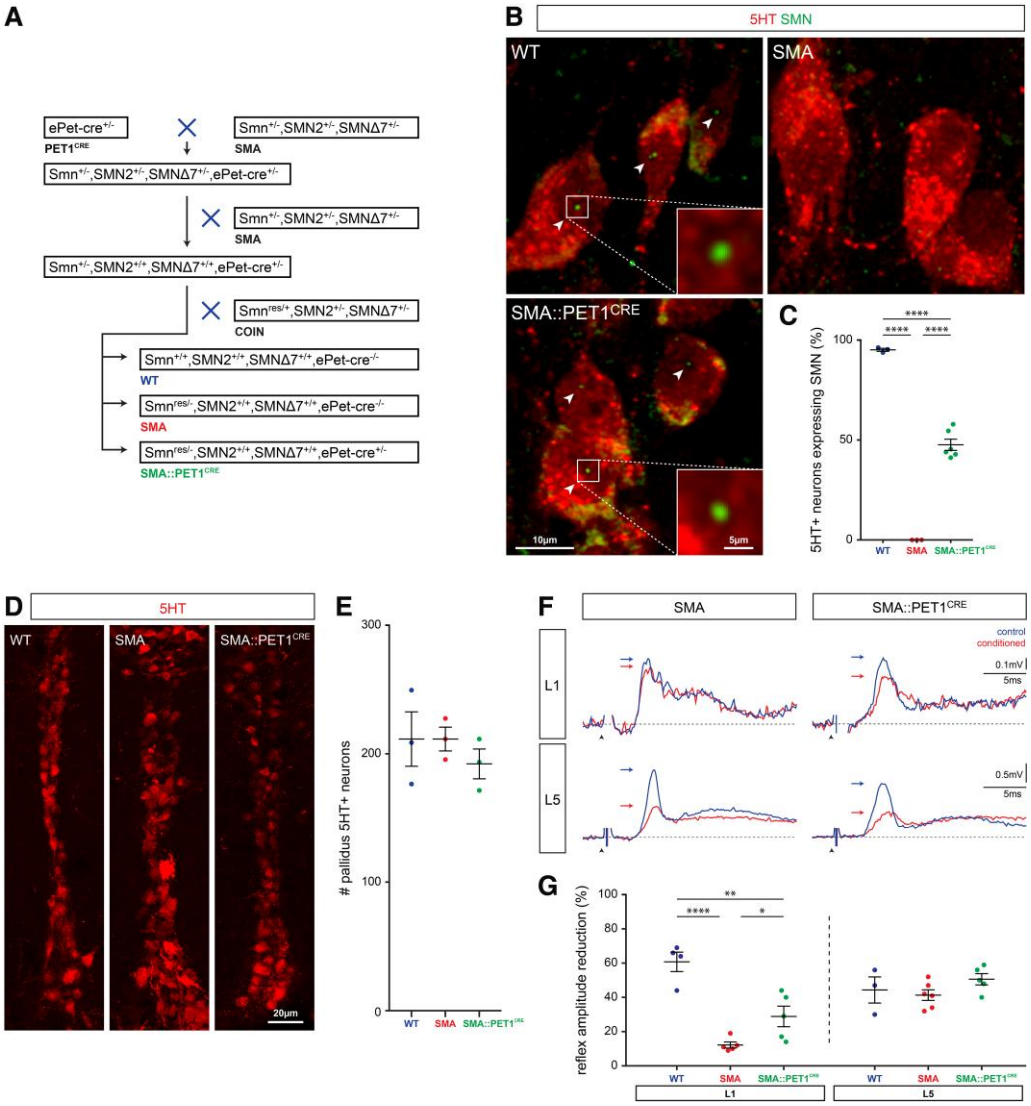

Figure 3 Genetic restoration of SMN selectively in raphe nuclei serotonergic neurons improves neuromodulation function in the spinal cord. (**A**) Diagram of the genetic strategy employed to restore SMN expression under the *Pet1* promoter in SMA mice. The '×' denotes mouse crosses. COIN = conditional inversion. (**B**) SMN immunoreactivity revealed as gems (green) in brainstem serotonergic neurons (red) in wild-type (WT), spinal muscular atrophy (SMA) and SMA::Pet1^{CRE}, at P10. No gems were observed in SMA mice. (**C**) Quantification of the proportion of serotonergic cells containing at least one SMN gem. WT: $N = 3$, SMA: $N = 3$, SMA::Pet1^{CRE}, $N = 6$; ANOVA, Tukey's *post hoc* test, WT versus SMA, $^{****}P < 0.0001$; WT versus SMA::Pet1^{CRE}, $^{****}P < 0.0001$; SMA versus SMA::Pet1^{CRE}, $^{****}P < 0.0001$. (**D**) 5-HT immunoreactivity of the raphe pallidus in wild-type, SMA and SMA::Pet1^{CRE} brainstems at P10. (**E**) Quantification of the number of 5-HT+ neurons in the ventral 300 µm area of the brainstem in WT, SMA and SMA::Pet1^{CRE} mice. WT: $N = 3$, SMA: $N = 3$, SMA::Pet1^{CRE}, $N = 3$; ANOVA, Tukey's *post hoc* test: WT versus SMA $P > 0.9999$; WT versus SMA::Pet1^{CRE}, $P = 0.6498$; SMA versus SMA::Pet1^{CRE}, $P = 0.6498$. (**F**) Responses of monosynaptic reflexes elicited in L1 and L5 spinal segments in SMA and SMA::Pet1^{CRE} mice, before (blue traces) and after (red traces) brainstem conditioning stimulation. (**G**) Quantification of the conditioning effect of serotonin (as percentage reduction) in the monosynaptic reflex for the three experimental groups. WT: L1, $N = 4$; SMA: L1, $N = 5$; SMA::Pet1^{CRE}: $N = 5$; ANOVA, Holm-Sidak *post hoc* test. Wild-type versus SMA, $^{****}P < 0.0001$; WT versus SMA::Pet1^{CRE}, $^{**}P = 0.0015$; SMA versus SMA::Pet1^{CRE}, $^{*}P = 0.0269$. WT: L5, $N = 3$; SMA: L5, $N = 6$; SMA::Pet1^{CRE}: $N = 5$; ANOVA, Holm-Sidak *post hoc* test, WT versus SMA, $P = 0.6398$; WT versus SMA::Pet1^{CRE}, $P = 0.5793$; SMA versus SMA::Pet1^{CRE}, $P = 0.2963$. N = number of mice; n = number of motor neurons.

Loss of 5-HT synapses in SMA involves C1q-dependent pathways

To delve into the molecular mechanisms responsible for serotonergic elimination, we investigated the potential involvement of C1q, the initiating protein of the classical complement cascade. We previously demonstrated that SMA proprioceptive synapses are eliminated through activation of the classical complement cascade and microglia engulfment.[42] Therefore, we quantified the tagging events by C1q on 5-HT^{+} synapses that contact somata of L1 motor neurons in wild-type, SMA and SMA::Pet1^{CRE} mice at P10. Z-stack of confocal images combined with image analysis using line-profile intensity measurements on single optical planes were used to define serotonergic synapses tagged by C1q (Fig. 5A and B). On the entire soma, we found a significant 3-fold increase of tagged 5-HT^{+} synapses in SMA (~23%) compared to wild-type mice, in which a relatively small percentage (~7%) exhibit C1q-tagging (Fig. 5C and D). Importantly, the C1q-tagging events on 5-HT synapses were significantly reduced in SMA::Pet1^{CRE} mice (~16%; Fig. 5C and D), revealing the serotonergic-autonomous nature of synaptic elimination. Taken

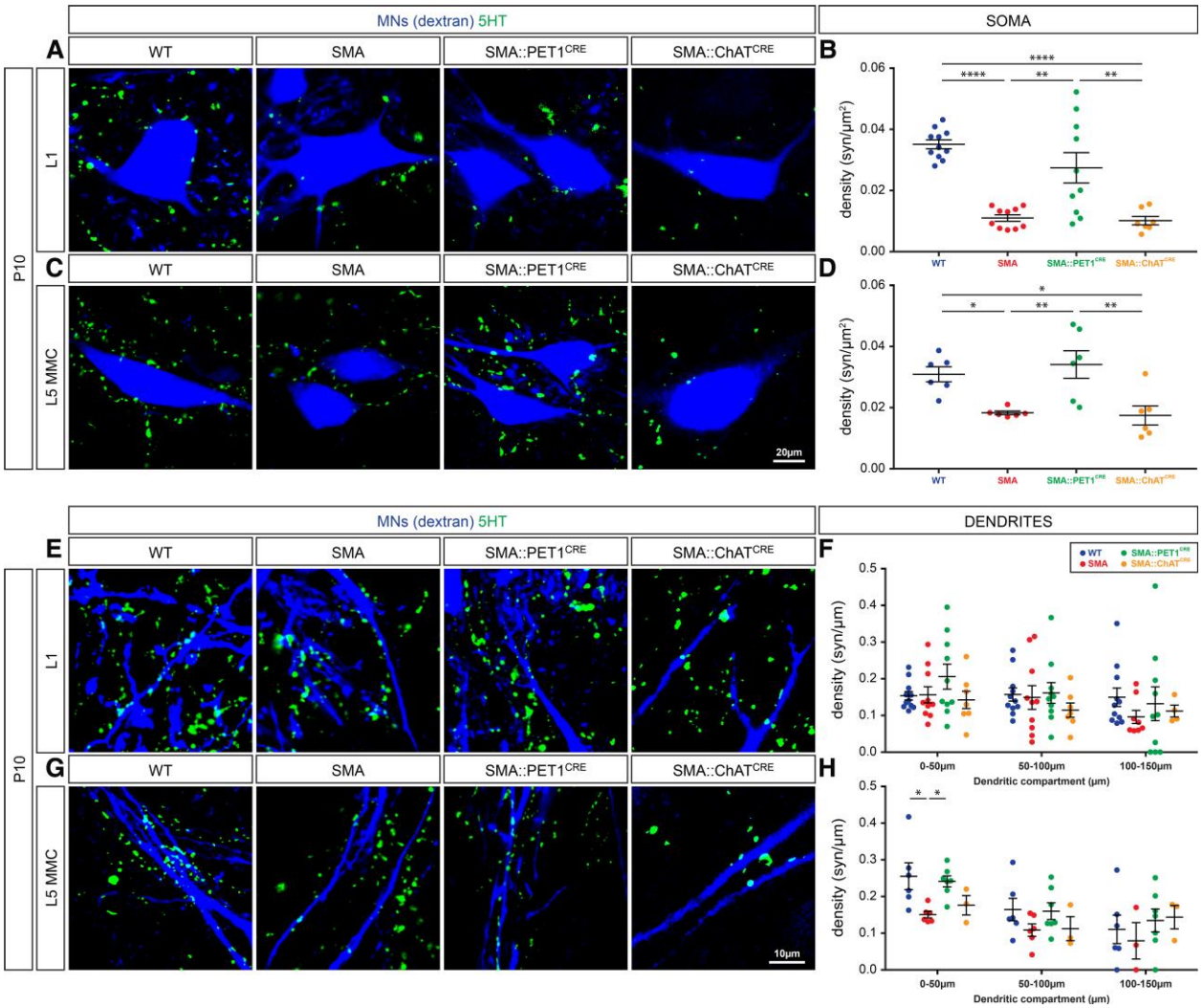

Figure 4 Serotonergic synaptic loss in SMA is mediated by serotonergic-autonomous mechanisms. (**A**) Z-stack projections (total: 5 µm) of confocal images of retrogradely filled wild-type (WT), spinal muscular atrophy (SMA), SMA::Pet1^{CRE} and SMA::ChAT^{CRE} L1 motor neurons (MNs, blue) and 5-HT+ synapses (green) at P10. (**B**) Quantification of the somatic 5-HT synaptic surface density in L1 motor neurons. *N* = number of mice; *n* = number of motor neurons. WT: *N* = 4, *n* = 11; SMA: N = 4, *n* = 10; SMA::Pet1^{CRE}: *N* = 4, *n* = 10; SMA::ChAT^{CRE}: *N* = 3, *n* = 7; ANOVA, Tukey's *post hoc* test. WT versus SMA, ****P < 0.0001; WT versus SMA::Pet1^{CRE}, *P* = 0.2077; WT versus SMA::ChAT^{CRE}, ****P < 0.0001; SMA versus SMA::Pet1^{CRE}, **P = 0.0011; SMA versus SMA::ChAT^{CRE}, *P* = 0.9971; SMA::Pet1^{CRE} versus SMA::ChAT^{CRE}, **P = 0.0018. (**C**) As in **A**, for L5-MMC motor neurons. (**D**) Quantification of the somatic 5-HT synaptic surface density in L5-MMC motor neurons. WT: *N* = 3, *n* = 6; SMA: *N* = 3, *n* = 6; SMA::Pet1^{CRE}: *N* = 3, *n* = 6; SMA::ChAT^{CRE}: *N* = 3, *n* = 7; ANOVA, Tukey's *post hoc* test. WT versus SMA, *P = 0.0408; WT versus SMA::Pet1^{CRE}, *P* = 0.8582; WT versus SMA::ChAT^{CRE}, *P = 0.0271; SMA versus SMA::Pet1^{CRE}, **P = 0.0073; SMA versus SMA::ChAT^{CRE}, *P* = 0.9973; SMA::Pet1^{CRE} versus SMA::ChAT^{CRE}, **P = 0.0047. (**E**) Z-stack projections (total: 2.75 µm) of confocal images from WT, SMA, SMA::Pet1^{CRE} and SMA::ChAT^{CRE} L1 motor neuron dendrites (blue) and 5-HT+ synapses (green) at P10. (**F**) Quantification of the 5-HT synaptic densities in the dendritic compartments 0–50, 50–100 and 100–150 µm from the soma from L1 motor neurons at P10. 0–50 µm: WT, *N* = 4, *n* = 11; SMA, *N* = 4, *n* = 10; SMA::Pet1^{CRE}, *N* = 4, *n* = 10; SMA::ChAT^{CRE}: *N* = 3, *n* = 7; ANOVA, Tukey's *post hoc* test. WT versus SMA, *P* = 0.9998; WT versus SMA::Pet1^{CRE}, *P* = 0.3887; WT versus SMA::ChAT^{CRE}, *P* = 0.9520; SMA versus SMA::Pet1^{CRE}, *P* = 0.4535; SMA versus SMA::ChAT^{CRE}, *P* = 0.9346; SMA::Pet1^{CRE} versus SMA::ChAT^{CRE}, *P* = 0.2092. 50–100 µm: WT, *N* = 4, *n* = 11; SMA, *N* = 4, *n* = 10; SMA::Pet1^{CRE}, *N* = 4, *n* = 10; SMA::ChAT^{CRE}: *N* = 3, *n* = 7; ANOVA, Tukey's *post hoc* test. WT versus SMA, *P* = 0.9956; WT versus SMA::Pet1^{CRE}, *P* = 0.9993; WT versus SMA::ChAT^{CRE}, *P* = 0.6916; SMA versus SMA::Pet1^{CRE}, *P* = 0.9858; SMA versus SMA::ChAT^{CRE}, *P* = 0.8172; SMA::Pet1^{CRE} versus SMA::ChAT^{CRE}, *P* = 0.6387. 100–150 µm: WT, *N* = 4, *n* = 11; SMA, *N* = 4, *n* = 8; SMA::Pet1^{CRE}, *N* = 4, *n* = 10; SMA::ChAT^{CRE}: *N* = 3, *n* = 4; ANOVA, Tukey's *post hoc* test. WT versus SMA, *P* = 0.6489; WT versus SMA::Pet1^{CRE}, *P* = 0.9759; WT versus SMA::ChAT^{CRE}, *P* = 0.9126; SMA versus SMA::Pet1^{CRE}, *P* = 0.8681; SMA versus SMA::ChAT^{CRE}, *P* = 0.9934; SMA::Pet1^{CRE} versus SMA::ChAT^{CRE}, *P* = 0.9858. (**G**) As in **E** for L5-MMC motor neurons at P10. (**H**) Quantification of the 5-HT longitudinal synaptic densities in the dendritic compartments 0–50, 50–100 and 100–150 µm from the soma for L5-MMC MNs. 0–50 µm: WT, *N* = 3, *n* = 6; SMA, *N* = 3, *n* = 6; SMA::Pet1^{CRE}, *N* = 3, *n* = 7; SMA::ChAT^{CRE}: *N* = 3, *n* = 3; ANOVA, Tukey's *post hoc* test. WT versus SMA, *P = 0.0214; WT versus SMA::Pet1^{CRE}, *P* = 0.9681; WT versus SMA::ChAT^{CRE}, *P* = 0.2249; SMA versus SMA::Pet1^{CRE}, *P = 0.0421; SMA versus SMA::ChAT^{CRE}, *P* = 0.9146; SMA::Pet1^{CRE} versus SMA::ChAT^{CRE}, *P* = 0.3608. 50–100 µm: WT, *N* = 3, *n* = 6; SMA, *N* = 3, *n* = 6; SMA::Pet1^{CRE}, *N* = 3, *n* = 7; SMA::ChAT^{CRE}: *N* = 3, *n* = 3; ANOVA, Tukey's *post hoc* test. WT versus SMA, *P* = 0.3965; WT versus SMA::Pet1^{CRE}, *P* = 0.9991; WT versus SMA::ChAT^{CRE}, *P* = 0.6192; SMA versus SMA::Pet1^{CRE}, *P* = 0.4356; SMA versus SMA::ChAT^{CRE}, *P* = 0.9997; SMA::Pet1^{CRE} versus SMA::ChAT^{CRE}, *P* = 0.6657. 100–150 µm: WT, *N* = 3, *n* = 6; SMA, *N* = 3, *n* = 3; SMA::Pet1^{CRE}, *N* = 3, *n* = 7; SMA::ChAT^{CRE}: *N* = 3, *n* = 3; ANOVA, Tukey's *post hoc* test. WT versus SMA, *P* = 0.9526; WT versus SMA::Pet1^{CRE}, *P* = 0.9547; WT versus SMA::ChAT^{CRE}, *P* = 0.9436; SMA versus SMA::Pet1^{CRE}, *P* = 0.7801; SMA versus SMA::ChAT^{CRE}, *P* = 0.7882; SMA::Pet1^{CRE} versus SMA::ChAT^{CRE}, *P* = 0.9986.

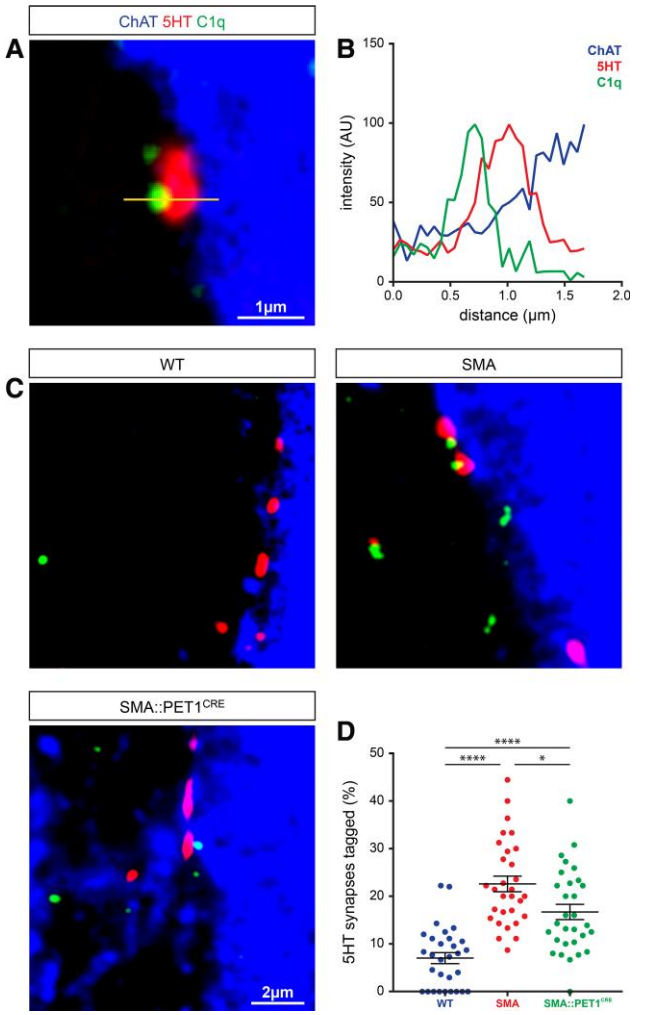

Figure 5 C1q 'tagging' of serotonergic synapses in SMA. (**A**) High-magnification confocal image of C1q (green) apposed to a putative 5-HT+ synapse (red) contacting a ChAT+ L1 motor neuron (blue). (**B**) Fluorescence intensity profile for C1q (green), 5-HT (red) and ChAT (blue) signals across the yellow line shown in **A**. Note the clear partial overlap between C1q and 5-HT. (**C**) Confocal images of C1q (green) and 5-HT+ synapses (red) on L1 wild-type (WT), spinal muscular atrophy (SMA) and SMA::Pet1^{CRE} ChAT+ motor neurons (blue) at P10. (**D**) Percentage of 5-HT synapses tagged by C1q on the somata of L1 WT, SMA and SMA::Pet1^{CRE} motor neurons at P10. *N* = number of mice; *n* = number of motor neurons. WT: *N* = 3, *n* = 30; SMA: *N* = 3, *n* = 30; SMA::Pet1^{CRE}: *N* = 3, *n* = 30; ANOVA, Tukey's *post hoc* test. WT versus SMA, ****$P < 0.0001$; WT versus SMA::Pet1^{CRE}, ****$P < 0.0001$; SMA versus SMA::Pet1^{CRE}, *$P = 0.0160$.

together, these results demonstrate that serotonergic synapses are reduced due to SMN deficiency in 5-HT neurons and that their elimination likely involves C1q-dependent mechanisms, similar to those observed for proprioceptive synapses.[42]

Selective restoration of SMN in serotonergic neurons does not affect motor neuron survival in SMA

The amplitude of the monosynaptic dorsal-to-ventral root response is mediated partly by the number of spinal motor neurons present in the spinal segment. To investigate whether death of SMA motor neurons is impacted by restoration of serotonergic neurotransmission in SMA::Pet1^{CRE} mice, we labelled spinal motor neurons with ChAT antibody and counted all the motor neurons in the L1 spinal segment, as previously described.[38] We found no significant improvement in rescue of L1 spinal motor neurons in SMA::Pet1^{CRE} mice compared to SMA mice (Fig. 6A and B). Furthermore, to investigate whether α and γ motor neurons are equally affected in SMA and SMA::Pet1^{CRE} mice, we performed measurements of the soma size in wild-type, SMA and SMA::Pet1^{CRE} mice at P10 in the L1 spinal segment (Fig. 6C). To differentiate between α and γ motor neurons, we identified motor neurons as α when the somatic maximal cross-section area was ≥400 µm^2, as previously reported.[72] Through distribution analysis we found that the large majority of SMA motor neurons destined to die are α-motor neurons, as they are the largest in soma size (Fig. 6D). Additionally, SMN restoration in 5-HT neurons did not reveal any significant difference between α and γ motor neurons when compared to SMA mice (Fig. 6D). These results indicate that SMN deficiency in serotonergic neurons does not influence the extent and types of motor neurons affected in SMA, in agreement with our previous report that motor neuron death is mediated by motor neuron-autonomous mechanisms involving p53 pathway activation.[73,74] Importantly, it rules out the possibility that the improvement in the reduction of the monosynaptic dorsal-to-ventral root reflex following conditioning by serotonergic neurons (Fig. 3F and G) is due to motor neuron rescue and therefore, it indicates that serotonergic neurotransmission is improved in SMA::Pet1^{CRE} mice.

Serotonergic and proprioceptive synapses are reduced independently of each other in SMA mice

Both proprioceptive and serotonergic synapses are lost in SMA mice and follow the same segment specific vulnerability. We therefore sought to investigate whether there is an inter-dependence between these two types of synapses under SMN-deficiency. To address this, we quantified the number of proprioceptive synapses, marked by VGluT1 immunoreactivity in wild-type, SMA and SMA::Pet1^{CRE} mice, in L1, L5 MMC and L5 LMC motor neurons at P10. Confocal microscopy analysis from Z-stack of confocal images revealed a large and significant reduction of VGluT1$^+$ synapses on the somata of both L1 (Fig. 7A and B) and L5 MMC motor neurons (Fig. 7D and E) in SMA mice, in agreement with our previous findings[38,39] and that of others.[49] However, proprioceptive synapses on SMA::Pet1^{CRE} L1 motor neurons revealed an unexpectedly small increase compared to SMA motor neurons (Fig. 7B and E). We next compared the synaptic density of both proprioceptive and serotonergic synapses in the soma of single L1 and L5 MMC motor neurons in either wild-type or SMA mice. We found that on average there is no clear difference between the density of VGluT1 and 5-HT synapses in L1 motor neurons (Fig. 7C), whereas in L5 MMC motor neurons, the density of serotonergic synapses was higher compared to the density of proprioceptive synapses for both wild-type and SMA (Fig. 7F). The conservation of the ratio between the two types of synapses and between wild-type and SMA for each motor pool, raises the possibility that the density of each synapse may be inter-dependent.

Since the largest percentage of proprioceptive synapses are found on the proximal dendrites of motor neurons,[39,75] we extended our investigations on motor neuron dendrites extending up to 150 µm away from the soma in dendritic compartments of 50 µm length. In SMA::Pet1^{CRE} mice, we found that there was no significant rescue of proprioceptive synapses in either L1 motor neuron dendrites (Fig. 7G and H) or in the L5 MMC motor neurons, at a late stage of disease (P10) (Fig. 7I and J). These results suggest that the reduction of proprioceptive and serotonergic synapses on SMA vulnerable motor neurons occurs independently of each other's influence.

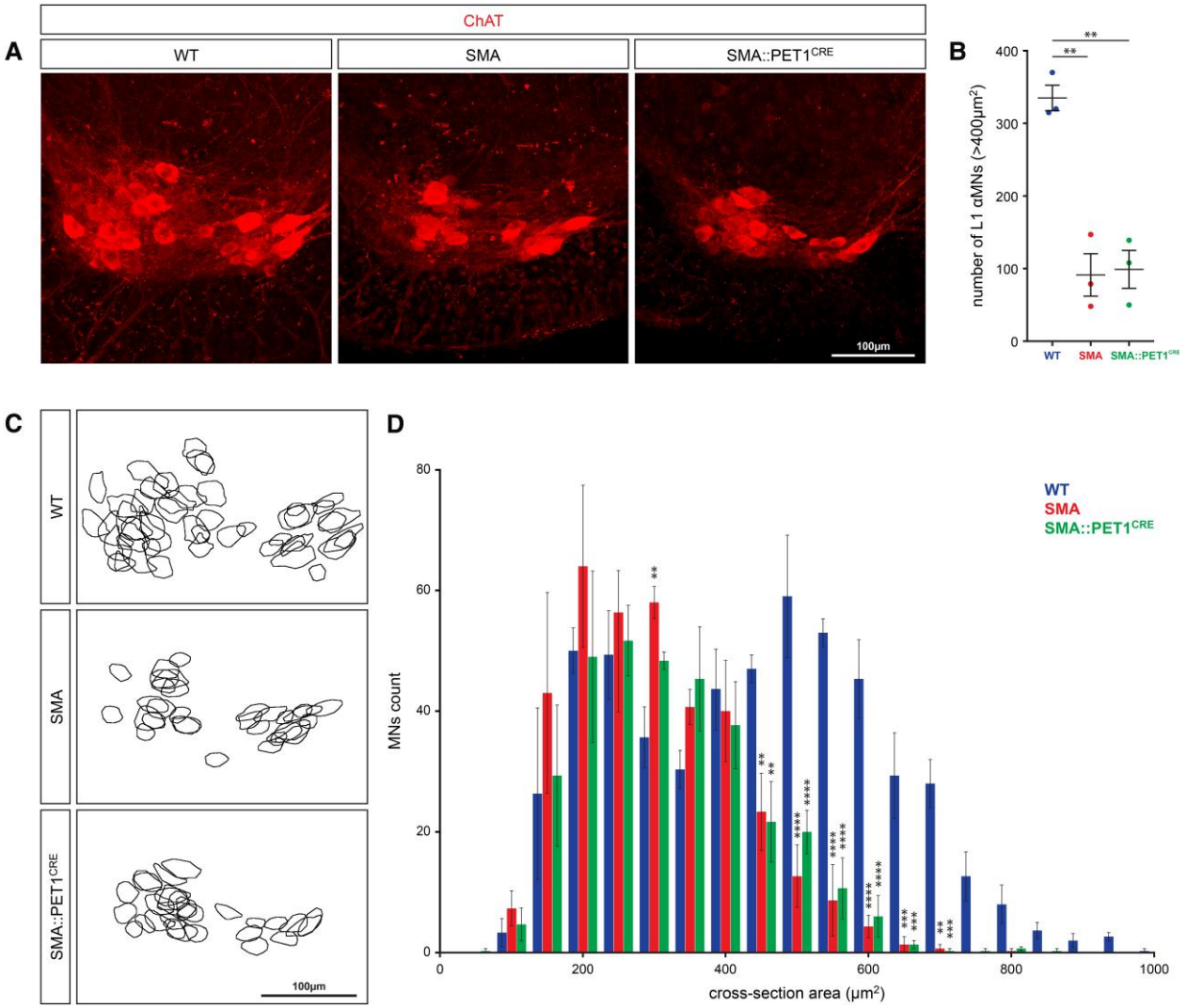

Figure 6 Selective SMN restoration in serotonergic neurons does not rescue vulnerable SMA motor neurons. (**A**) Z-stack projection (total: 75 µm) of confocal images showing ChAT immunoreactivity in the L1 ventral horn from wild-type (WT), spinal muscular atrophy (SMA) and SMA::Pet1^{CRE} mice. (**B**) Number of α motor neurons (soma cross-section area >400 µm^2) in the L1 segment for the three experimental groups at P10. WT: $N = 3$, SMA: $N = 3$, SMA::Pet1^{CRE}: $N = 3$; ANOVA, Tukey's *post hoc* test, WT versus SMA, $^{**}P = 0.0011$; WT versus SMA::Pet1^{CRE}, $^{**}P = 0.0013$; SMA versus SMA::Pet1^{CRE}, $P = 0.9741$. (**C**) Somata contours of ChAT+ motor neurons from the spinal sections depicted in **A**. (**D**) Histogram of motor neuron surface areas in WT (blue), SMA (red) and SMA::Pet1^{CRE} (green) located in the L1 segment at P10. WT: $N = 3$, SMA: $N = 3$, SMA::Pet1^{CRE}: $N = 3$; two-way ANOVA, Tukey's *post hoc* test; bin 300 µm^2: WT versus SMA, $^{**}P = 0.0099$; bin 450 µm^2: WT versus SMA, $^{**}P = 0.0058$, WT versus SMA::Pet1^{CRE}, $^{**}P = 0.0028$; bin 500 µm^2: WT versus SMA, $^{****}P < 0.0001$; WT versus SMA::Pet1^{CRE}, $^{****}P < 0.0001$; bin 550 µm^2: WT versus SMA, $^{****}P < 0.0001$; WT versus SMA::Pet1^{CRE}, $^{****}P < 0.0001$; bin 600 µm^2: WT versus SMA, $^{****}P < 0.0001$; WT versus SMA::Pet1^{CRE}, $^{****}P < 0.0001$; bin 650 µm^2: WT versus SMA, $^{***}P = 0.0008$; WT versus SMA::Pet1^{CRE}, $^{***}P = 0.0008$; bin 700 µm^2: WT versus SMA, $^{**}P = 0.0012$; WT versus SMA::Pet1^{CRE}, $^{***}P = 0.0010$. N = number of mice; n = number of motor neurons.

Serotonin has been associated with the proliferation and refinement of network connections during normal development in several CNS regions, including the somatosensory cortex and the respiratory centres.[13] It is possible that in spinal motor circuits, serotonin may exert a similar trophic or protective effect on the proprioceptive synapses that could operate in a microscale. If such an effect exists, we would expect a selective pruning of proprioceptive synapses that are the most distant to serotonergic ones, resulting in the formation of clusters of proprioceptive synapses around serotonergic ones during normal development. To explore this hypothesis, we analysed our results by calculating the nearest neighbour index for VGluT1 synapses toward the 5-HT synapses [Rn, Fig. 7M and Equation (1)]. A Rn inferior to 1 would indicate a cluster distribution around 5-HT synapses. Neurolucida reconstructed motor neurons receiving proprioceptive (VGluT1$^+$) and serotonergic (5-HT$^+$) synapses on the L1 (Fig. 7K, N and O) and L5 MMC (Fig. 7L, P and Q) motor neurons revealed that there is no statistically significant influence of serotonergic synapses on neighbouring proprioceptive synapses, indicating that: (i) serotonin does not have a trophic effect on the localization of proprioceptive synapses in normal development; and (ii) proprioceptive synapses are reduced randomly in SMA and do not benefit from any protective effect by the proximity of 5-HT synapses.

Combined SMN restoration in serotonergic and motor neurons improves righting and lifespan in SMA

One of the hallmark behavioural deficits in SMA mice is the inability to right, similar to the inability of rolling in SMA type I patients. This

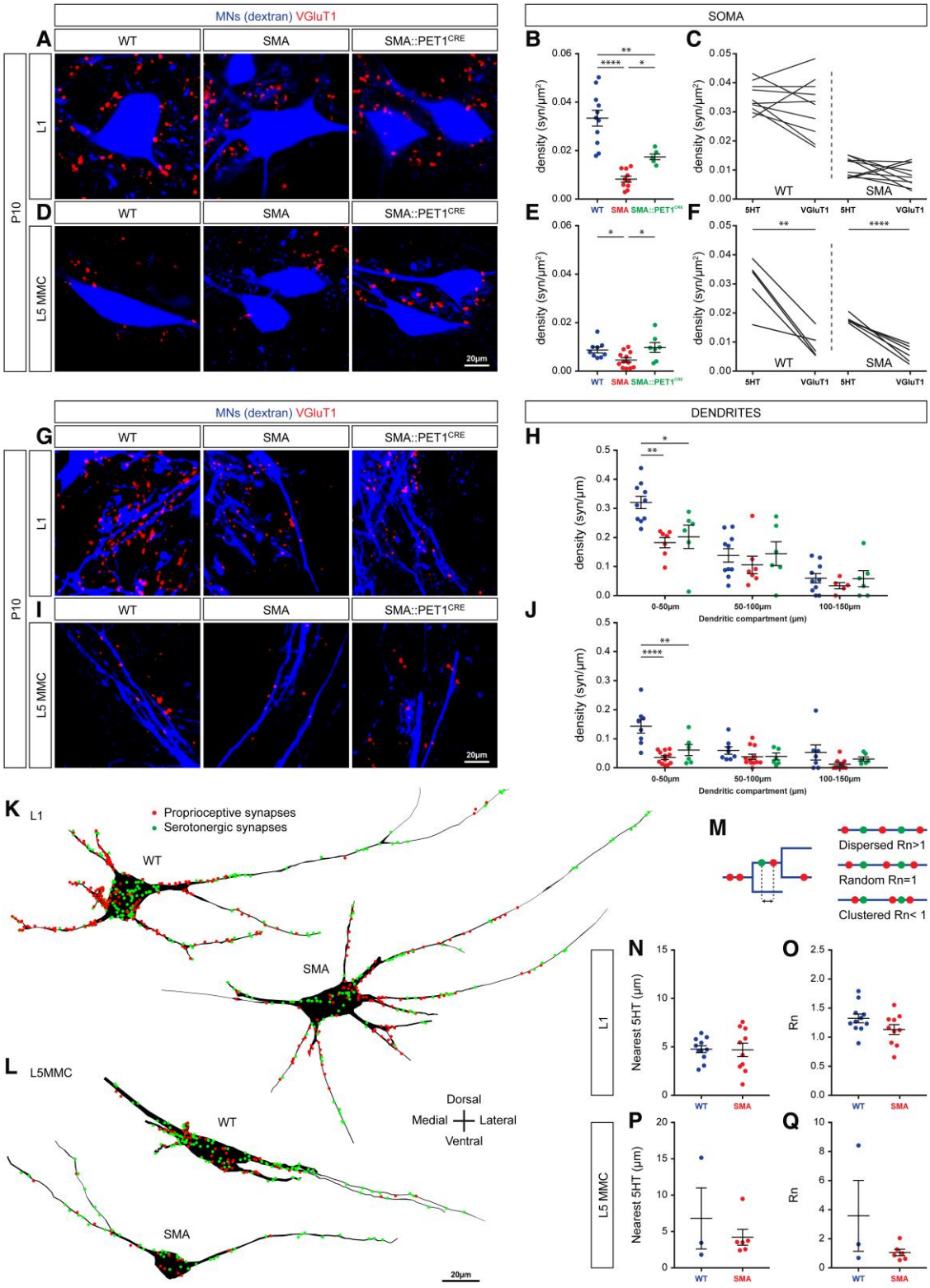

Figure 7 5-HT+ and VGluT1+ synapses are reduced independently of each other in SMA. (**A**) *Z*-stack projections (total: 5 µm) of confocal images of retrogradely filled wild-type (WT), spinal muscular atrophy (SMA) and SMA::Pet1^{CRE} L1 motor neurons (MNs, blue) and VGluT1 synapses (red) at P10. (**B**) Quantification of the somatic VGluT1 synaptic surface density in L1 motor neurons. *N* = number of mice; *n* = number of motor neurons. WT: $N = 4$, $n = 11$; SMA: $N = 4$, $n = 10$; SMA::Pet1^{CRE}: $N = 4$, $n = 5$; ANOVA, Holm-Sidak *post hoc* test. WT versus SMA, $^{****}P < 0.0001$; WT versus SMA::Pet1^{CRE}, $^{**}P = 0.0017$; SMA versus SMA::Pet1^{CRE}, $^{*}P = 0.0364$. (**C**) Comparison of 5-HT and VGluT1 soma synaptic densities for WT and SMA L1 motor neurons. The lines link values for the same motor neuron. WT: $N = 4$, $n = 10$; *t*-test with Welch's correction, $P = 0.6612$. Pearson correlation $r = 0.4560$, $P = 0.1586$. SMA: $N = 4$, $n = 10$; *t*-test with Welch's correction, $P = 0.1045$. Pearson correlation $r = -0.2398$, $P = 0.5046$. (**D**) As in **A** for L5-MMC motor neurons (blue) and VGluT1 synapses (red) at P10. (**E**) Quantification of the somatic VGluT1 synaptic surface density in L5-MMC motor neurons. WT: $N = 9$, $n = 5$; SMA: $N = 4$, $n = 12$; SMA::Pet1^{CRE}: $N = 4$, $n = 7$; ANOVA, Holm-Sidak *post hoc* test. WT versus SMA, $^{*}P = 0.0433$; WT versus SMA::Pet1^{CRE}, $P = 0.6464$; SMA

(continued)

is partly due to impairment of sensory-motor circuits manifested by dysfunction of proprioceptive synapses and motor neurons loss innervating vulnerable muscles under SMN deficiency. We investigated whether selective restoration of SMN in serotonergic neurons has any effects on motor behaviour, body weight or survival in wild-type, SMA and SMA::Pet1^{CRE} mice. We found no significant improvement in weight gain (Supplementary Fig. 5A) or righting time (Supplementary Fig. 5B). We also tested whether serotonergic transmission might influence posture in the three groups of mice but found that SMA::Pet1^{CRE} mice exhibited similar deficits in posture to those observed in SMA mice (Supplementary Fig. 5C), indicating that serotonergic transmission does not play a major role in these behavioural traits. Finally, no benefits were observed in the lifespan between SMA::Pet1^{CRE} and SMA mice (Supplementary Fig. 5D).

The behavioural benefits provided by SMN restoration in serotonergic neurons could be masked by the degeneration of the motor neurons themselves during the time course of the disease. To reveal those potential benefits, we crossed our SMA::Pet1^{CRE} line with the SMA::ChAT^{CRE} mice in which restoration of SMN in ChAT positive neurons rescues motor neurons from degeneration, improves righting time and extends survival.[39] Following this strategy, SMA::(Pet1+ChAT)^{CRE} showed further improved righting time (Supplementary Fig. 5E) and extended survival by an average of 2 days (Supplementary Fig. 5F) compared to the SMA::ChAT^{CRE} mice, indicating that SMN restoration in serotonergic neurons have mild but significant benefits in behaviours affected by SMA.

SMN restoration in serotonergic neurons facilitates interlimb coordination during *in vivo* locomotion

Serotonergic neurotransmission plays an important role in fine tuning spinal circuits involved in various motor behaviours.[76] To this end, it has been established that serotonin contributes to the regulation of locomotor rhythm[6,21] and the duration of muscle contraction, as well as stabilization of inter-limb coordination during free movement.[77] To uncover the importance of serotonergic dysfunction in SMA, we recorded muscle activity from the tibialis anterior muscle bilaterally, during voluntary locomotion *in vivo* in wild-type (Fig. 8A), SMA (Fig. 8B) and SMA::Pet1^{CRE} mice (Fig. 8C), at P10. We found that the left–right coordination was significantly reduced in SMA mice (Fig. 8E and H) compared to wild-type mice (Fig. 8D and G), as demonstrated by an increase of cycle phase variability and a significantly reduced r-score compared to control littermates (Fig. 8J). In contrast, neither the locomotor cycle duration (Fig. 8K), nor the bout duration of the muscle activity (Fig. 8L) were significantly affected in SMA, despite a trend for an increase in both parameters in SMA mice. Strikingly, selective SMN restoration in serotonergic neurons (SMA::Pet1^{CRE} mice), rescued entirely the left–right coordination in SMA mice, bringing to wild-type levels during locomotion (Fig. 8F, I and J) without affecting the cycle duration or the bout duration (Fig. 8K and L). To test the locomotor behaviour in muscles innervated by motor neurons in the vulnerable rostral lumbar segments (L1-L2), we recorded EMG activity from the psoas muscles, which are innervated by L1/L2 motor neurons.[39] Despite the large extent of NMJ denervation in the iliopsoas muscles in SMA mice, we were able to conduct *in vivo* experiments at P10 (Supplementary Fig. 6A–C). We observed similar results in psoas muscles as from tibialis anterior muscles. The left–right coordination was significantly reduced in SMA psoas muscles (Supplementary Fig. 6E and H) compared to wild-type mice (Supplementary Fig. 6D and G), as reflected by an increase of cycle phase variability and a reduced r-score (Supplementary Fig. 6J). Finally, selective SMN restoration in serotonergic neurons of SMA mice (SMA::Pet1^{CRE} mice), improved drastically the left–right coordination (Supplementary Fig. 6F and I). The cycle and bout durations were similar among the three groups (Supplementary Fig. 6K and L). Taken together, these results demonstrate that impaired serotonergic neuromodulation results in significant dysfunction of interlimb coordination during free movement in SMA mice. Moreover, locomotor coordination being affected similarly for muscles innervated by vulnerable (psoas) and resistant (tibialis anterior) motor neurons suggests that serotonergic dysfunction in SMA impacts not only motor neurons but the spinal locomotor network.

Discussion

Our findings that serotonergic transmission is severely compromised in SMA mice uncover an unexpected role of SMN in

Figure 7 (Continued)
versus SMA::Pet1^{CRE}, *$P = 0.0317$. (**F**) Comparison of 5-HT and VGluT1 soma synaptic densities for WT and SMA L5-MMC motor neurons. The lines link values for the same motor neuron. WT: $N = 4$, $n = 5$; *t*-test with Welch's correction, $P = 0.0030$. Pearson correlation $r = 0.1420$, $P = 0.8199$. SMA: $N = 4$, $n = 6$; *t*-test with Welch's correction, $P < 0.0001$. Pearson correlation $r = –0.2641$, $P = 0.6130$. (**G**) Z-stack projections (total: 2.75 µm) of confocal images from WT, SMA and SMA::Pet1^{CRE} L1 motor neuron dendrites (blue) and VGluT1 synapses (green) at P10. (**H**) Quantification of the VGluT1 synaptic densities in the dendritic compartments 0–50, 50–100 and 100–150 µm from the soma for L1 motor neurons. 0–50 µm: WT, $N = 4$, $n = 10$; SMA, $N = 4$, $n = 7$; SMA::Pet1^{CRE}, $N = 4$, $n = 6$; ANOVA, Tukey's *post hoc* test. WT versus SMA, **$P = 0.0024$; WT versus SMA::Pet1^{CRE}, *$P = 0.0122$; SMA versus SMA::Pet1^{CRE}, $P = 0.8711$. 50–100 µm: WT, $N = 4$, $n = 10$; SMA: $N = 4$, $n = 7$; SMA::Pet1^{CRE}, $N = 4$, $n = 6$; ANOVA, Tukey's *post hoc* test. WT versus SMA, $P = 0.7066$; WT versus SMA::Pet1^{CRE}, $P = 0.9889$; SMA versus SMA::Pet1^{CRE}, $P = 0.6821$. 100–150 µm: WT, $N = 4$, $n = 10$; SMA, $N = 4$, $n = 7$; SMA::Pet1^{CRE}, $N = 4$, $n = 6$; ANOVA, Tukey's *post hoc* test. WT versus SMA, $P = 0.6425$; WT versus SMA::Pet1^{CRE}, $P = 0.9979$; SMA versus SMA::Pet1^{CRE}, $P = 0.7268$. (**I**) As in **G** for L5-MMC motor neuron dendrites at P10. (**J**) Quantification of the VGluT1 synaptic densities in the dendritic compartments 0–50, 50–100 and 100–150 µm from the soma for L5-MMC motor neurons. 0–50 µm: WT, $N = 4$, $n = 8$; SMA, $N = 4$, $n = 12$; SMA::Pet1^{CRE}, $N = 3$, $n = 6$; ANOVA, Tukey's *post hoc* test. WT versus SMA, ****$P < 0.0001$; WT versus SMA::Pet1^{CRE}, **$P = 0.0065$; SMA versus SMA::Pet1^{CRE}, $P = 0.5752$. 50–100 µm: WT, $N = 4$, $n = 8$; SMA, $N = 4$, $n = 12$; SMA::Pet1^{CRE}, $N = 3$, $n = 6$; ANOVA, Tukey's *post hoc* test. WT versus SMA, $P = 0.3108$; WT versus SMA::Pet1^{CRE}, $P = 0.3239$; SMA versus SMA::Pet1^{CRE}, $P = 0.9737$. 100–150 µm: WT, $N = 4$, $n = 7$; SMA, $N = 4$, $n = 9$; SMA::Pet1^{CRE}, $N = 3$, $n = 6$; ANOVA, Tukey's *post hoc* test. WT versus SMA, $P = 0.1533$; WT versus SMA::Pet1^{CRE}, $P = 0.5709$; SMA versus SMA::Pet1^{CRE}, $P = 0.7199$. (**K**) 3D reconstruction of L1 WT and SMA motor neurons with their dendritic tree contained in a 75 µm-thick transverse spinal section. 5-HT synapses are represented by green dots and VGluT1 synapses by red dots. (**L**) Similar 3D reconstructions for L5-MMC WT and SMA motor neurons. (**M**) Illustration showing the measure of the average minimal distances between the two different types of synapses used for the nearest neighbour (Rn; see 'Materials and methods' section for calculation) analysis (NNA, *left*) and the three possible types of distributions according to the Rn score calculated (*right*). (**N**) Quantification of the average distance of the nearest 5-HT synapse from each VGluT1 synapse in L1 motor neuron dendrites for WT and SMA animals. WT: $N = 4$, $n = 10$; SMA: $N = 4$, $n = 10$; *t*-test with Welch's correction, $P = 0.9282$. (**O**) Rn score from NNA for WT and SMA L1 motor neurons. WT: $N = 4$, $n = 10$; SMA: $N = 4$, $n = 10$; *t*-test with Welch's correction, $P = 0.1065$. (**P**) Quantification of the average distance of the nearest 5-HT synapse from each VGluT1 synapse in L5-MMC motor neuron dendrites for WT and SMA animals. WT: $N = 3$, $n = 3$; SMA: $N = 3$, $n = 6$; Mann-Whitney-Wilcoxon test, $P = 0.9048$. (**Q**) Rn score from NNA for WT and SMA L5-MMC motor neurons. WT: $N = 3$, $n = 3$; SMA: $N = 3$, $n = 6$; Mann-Whitney-Wilcoxon test, $P = 0.4102$.

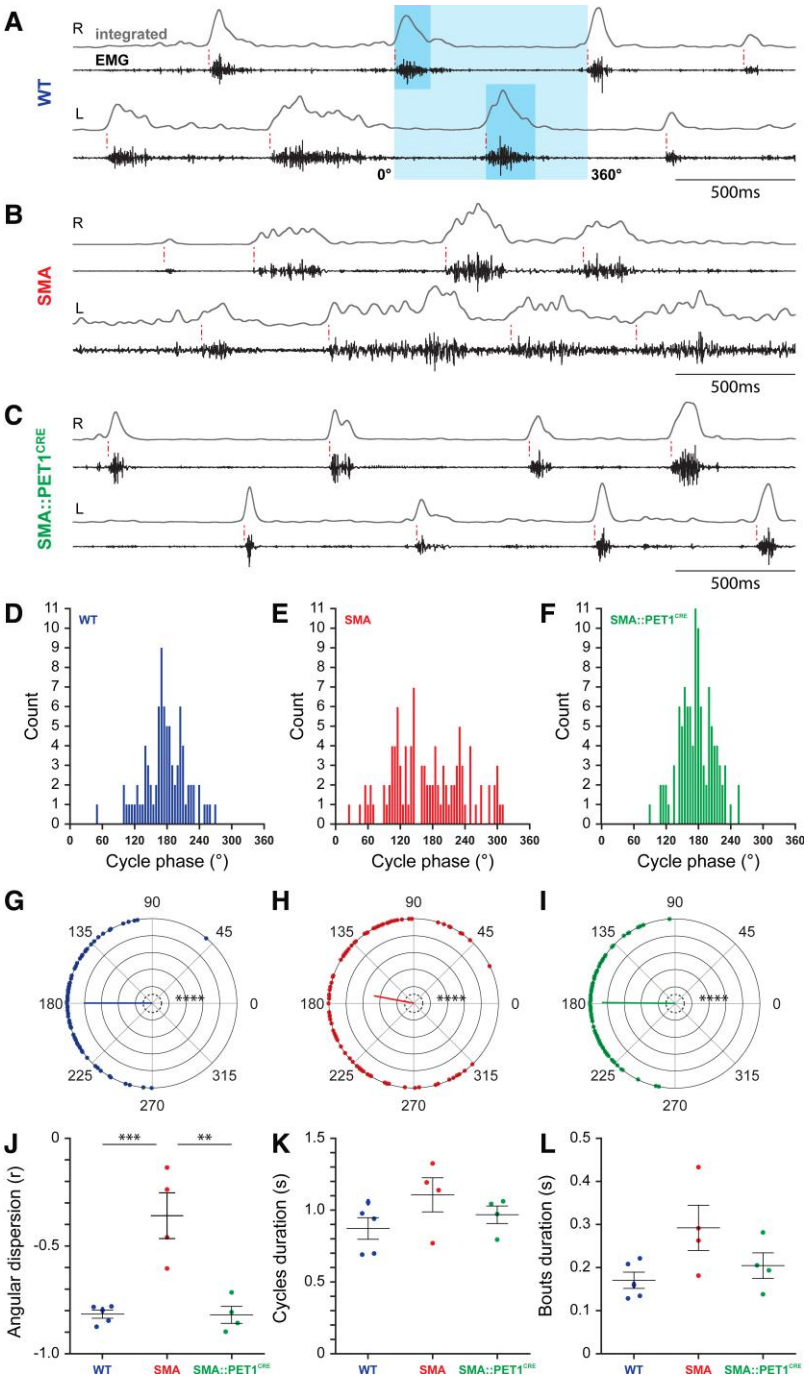

Figure 8 Perturbations in locomotor activity in SMA mice are rescued after selective SMN restoration in serotonergic cells. (**A**) Bilateral recordings from tibialis anterior (TA) EMG activity in a wild-type (WT) mouse during locomotion at P10. Black traces show the raw recordings, grey traces display the rectified and filtered signals. The dotted vertical red lines show the beginning of each bout of TA activity in both legs. The box highlighted in blue depicts a full cycle of locomotor activity (0 to 360°) locked on the right TA. Dark blue periods correspond to bouts of TA activity during the swing phase for each leg, light blue periods correspond to periods of TA rest during the stance phase. (**B**) As in **A** in a P10 spinal muscular atrophy (SMA) mouse. (**C**) As in **A** and **B** in a P10 SMA::Pet1^{CRE} mouse. Distribution of right–left cycles phase alternation for the WT (**D**), SMA (**E**) and SMA::Pet1^{CRE} (**F**) mouse as shown in **A**, **B** and **C**, respectively. The corresponding polar plots in WT (**G**), SMA (**H**) and SMA::Pet1^{CRE} (**I**). The bar corresponds to the mean vector *r*. The vector length represents the left-right alternation strength, and the vector angle indicates the average alternation phase shift between the two legs. *N* = number of mice; *n* = number of cycles. WT: $N = 5$, $n = 288$, Rayleigh test, $P < 0.0001$; SMA: $N = 4$, $n = 329$, Rayleigh test, $P < 0.0001$; SMA::Pet1^{CRE}: $N = 4$, $n = 422$, Rayleigh test, $P < 0.0001$. (**J**) The angular dispersion represents the mean vector length measured for each animal in WT, SMA and SMA::Pet1^{CRE} mice. Wolraff test, $P < 0.0001$; ANOVA, Tukey's *post hoc* test. WT versus SMA, $^{***}P = 0.0009$; WT versus SMA::Pet1^{CRE}, $P = 0.9717$; SMA versus SMA::Pet1^{CRE}, $^{**}P = 0.0009$. (**K**) Mean cycle duration. WT: $N = 5$; SMA: $N = 4$; SMA::Pet1^{CRE}: $N = 4$; ANOVA, Tukey's *post hoc* test. WT versus SMA, $P = 0.2257$; WT versus SMA::Pet1^{CRE}, $P = 0.5149$; SMA versus SMA::Pet1^{CRE}, $P = 0.5149$. (**L**) Mean bout duration. WT: $N = 5$; SMA: $N = 4$; SMA::Pet1^{CRE}: $N = 4$; ANOVA, Tukey's *post hoc* test. WT versus SMA, $P = 0.0687$; WT versus SMA::Pet1^{CRE}, $P = 0.7615$; SMA versus SMA::Pet1^{CRE}, $P = 0.2388$.

neuromodulation. Serotonergic synapses in vulnerable spinal segments from SMA mice exhibit significant dysfunction early in the disease process. The dysfunctional 5-HT synapses are subsequently and progressively reduced in number both on the somata and dendrites of motor neurons innervating axial and proximal muscles, which are vulnerable and clinically relevant in SMA patients. Importantly, dysfunction and reduction of 5-HT synapses are due to the effects of SMN deficiency in serotonergic neurons. The behavioural significance of the deficits in serotonergic neurotransmission is reflected by interlimb incoordination that becomes apparent at late stages of mouse postnatal development.

5-HT receptors are widely expressed in spinal cord[61,78,79] and serotonin synapses make numerous contacts with the soma and dendrites of spinal motor neurons.[80] The effects of 5-HT on motor neurons include depolarization and increased excitability,[79] as well as inhibitory effects.[81,82] In view of this ambiguity, we tested serotonergic transmission in neonatal spinal cords, by examining the effects of 5-HT on the monosynaptic dorsal-to-ventral root reflex following electrical stimulation of the raphe nuclei. The monosynaptic reflex has been well established to be reduced during 5-HT exposure.[64,65,83–85] The reduction of the reflex is thought to be attributed to serotonergic receptors on sensory primary afferents[62,66,86–88] and not due to direct effects on motor neuron excitability.[64,83] Our results are in agreement with the reduction of the monosynaptic reflex following conditioning by electrical stimulation of the raphe nuclei in wild-type mice. Importantly, we validated pharmacologically that this reduction was serotonergically mediated. Furthermore, optical activation of 5-HT$^+$ neurons expressing ChR2 by photoillumination demonstrated that the effects of electrical stimulation on the reduction of the monosynaptic reflex were due to serotonin release. Therefore, the absence of reduction in the monosynaptic reflex in SMA mice demonstrates that serotonergic neurotransmission is defective in the spinal cord at the onset and late stages of disease, in agreement with a previous report showing reduced neuronal activity in SMA spinal cord after 5-HT exposure.[89]

Dysfunction of serotonergic transmission precedes 5-HT synaptic removal, with motor neurons innervating proximal and axial muscles being preferentially affected. Serotonergic SMA synapses were reduced in number as the disease progressed, reminiscent of the loss of proprioceptive synapses in vulnerable motor neurons.[38,39] The dysfunction and subsequent loss of 5-HT synapses occurs within serotonergic neurons because selective restoration of SMN in *Pet1*$^+$ serotonergic neurons rescued these events, while SMN restoration in *ChAT*$^+$ motor neurons didn't provide any protection. The less than complete rescue of 5-HT synapses is likely due to the partial efficiency of CRE to genetically restore SMN protein in ~50% of 5-HT neurons. Additionally, the reduction in serotonergic synaptic coverage on vulnerable motor neurons was not due to death of 5-HT neurons. Instead, serotonergic neurons exhibit progressive synaptic dysfunction and elimination of synapses that likely involves activation of microglia and the aberrant activation of the classical complement cascade. This interpretation is based on the significantly greater 'tagging' events by C1q on 5-HT$^+$ synapses contacting vulnerable motor neurons. C1q, the initiating protein of the classical complement cascade, is causally responsible for the elimination of proprioceptive synapses on vulnerable motor neurons in SMA mice.[42] Thus, C1q-dependent mechanisms are likely responsible for synaptic removal, raising the possibility that shared mechanisms of removal of 5-HT and proprioceptive synapses are in operation in mouse models of SMA.[42] Additionally, dysfunction in *Stasimon* in 5-HT neurons, a downstream target of SMN, may also be involved in this process, similar to the loss of proprioceptive synapses.[44] Selective restoration of SMN in serotonergic neurons did not improve motor neuron death due to SMN deficiency, providing further support to our previous findings that motor neuron death in SMA mice is caused by different cell autonomous mechanisms.[44,73,74]

5-HT projections from a single neuron or nucleus of serotonergic neurons are known to innervate several synaptically interconnected neuronal targets.[90,91] However, in the ventral horn of the spinal cord, 5-HT synapses preferentially innervate motor neurons projecting to axial rather than distal musculature.[92] In our study, we have observed significantly reduced 5-HT synaptic coverage in L5 MMC motor neurons, which innervate axial musculature such as multifidus and longissimus lumborum [the motor neurons innervating these muscles span from the L2-L6 spinal segments in the cat[93] and L1-L5 in the mouse (this study)]. The significance of this finding may help explain the proximo-distal course of the disease in the musculature affected, which is observed both in mice[39] and in human patients.[94,95] Scoliosis develops in nearly all children with type I SMA who are untreated medically[96] and becomes more severe once SMA patients become non-ambulatory.[97] Although serotonin itself does not result directly in motor neuron firing, its modulation enhances their repetitive firing ability.[60,98–102] Thus, if there are fewer or dysfunctioning 5-HT synapses on MMC motor neurons, this may lead to severe impairment of motor neuron firing, resulting in compromised contraction of axial muscles, possibly leading to scoliosis in SMA patients.[103] Furthermore, motor neuron function may also be benefited by serotonin, since activation of 5-HT$_{2A}$ in motor neurons has been shown to increase the cell membrane expression of KCC2, which may have therapeutic potential in the treatment of neurological disorders involving altered chloride homeostasis.[104]

SMA mice have been reported not to exhibit an impairment of locomotor-like activity at disease onset.[105] Here, we investigated locomotor behaviour at a late stage of the disease and found that the locomotor pattern was greatly affected by changes in interlimb coordination. Our results are consistent with previous studies in which serotonin was pharmacologically or surgically reduced, leading to major effects on intra- and interlimb coordination.[106–108] The significance of our results on the clinical impact for SMA patients is underlined by well established mobility issues, decreased endurance and gait impairments reported in SMA patients.[109,110] Additionally, spinal deformity such as scoliosis together with diminishing interlimb coordination leads to significant impairments of limb movement, trunk stability and gait.[111] Furthermore, the clinical significance of our findings of the dysregulated serotonergic neuromodulation of locomotor activity in SMA may be relevant to other rhythmic behaviours, such as suckling, chewing, feeding and breathing, which are all affected in SMA patients and mouse models of the disease. Finally, serotonergic dysfunction may also have implications in mood disorders in SMA patients, as has been reported recently.[112] In summary, the severe dysfunction in serotonergic neuromodulation in SMA mice provides important insights in the disease mechanisms and sheds light into both the proximo-distal disease progression and the dysregulation of locomotor behaviour observed in SMA. Our study suggests that the proper function of serotonergic neurotransmission in neuronal networks plays a critical role and should be considered a major therapeutic target, if normal function is to be restored in spinal muscular atrophy.

Data availability

The authors confirm that the data supporting the findings of this study are available within the article and its Supplementary

material. Any raw data (images and recordings) will be shared by the corresponding author upon reasonable request. This study did not generate any large datasets.

Acknowledgements

We would like to thank Drs Livio Pellizzoni, Michael O'Donovan, Daniel Zytnicki, Francesco J. Alvarez and members of the Mentis Lab for critical comments and suggestions on the manuscript. We also thank Dr Rene Hen for his kind gift of the Pet1^{CRE} mice. We thank Dr F. J. Alvarez for help with NeuroLucida analysis. We also want to thank Mr Geo Ables for technical assistance in genotyping and mouse husbandry.

Funding

G.Z.M. is supported by NINDS, NIH (R01-NS078375), The NIH Blueprint for Neuroscience Research (R01-AA027079), The SMA Foundation, and Project-ALS. N.D. is supported by AFM Téléthon.

Competing interests

The authors report no competing interests.

Supplementary material

Supplementary material is available at *Brain* online.

References

1. Curragh EF. The state of consciousness and very high frequency signalling in the serotonergic neuronal system. *J Physiol Paris*. 1997;91:69-73.
2. Grimaldi B, Fillion G. 5-HT-moduline Controls serotonergic activity: Implication in neuroimmune reciprocal regulation mechanisms. *Prog Neurobiol*. 2000;60:1-12.
3. Nalivaiko E, Blessing WW. Potential role of medullary raphe-spinal neurons in cutaneous vasoconstriction: An in vivo electrophysiological study. *J Neurophysiol*. 2002;87:901-911.
4. Ootsuka Y, Blessing WW. Inhibition of medullary raphé/parapyramidal neurons prevents cutaneous vasoconstriction elicited by alerting stimuli and by cold exposure in conscious rabbits. *Brain Res*. 2005;1051:189-193.
5. Gross C, Hen R. The developmental origins of anxiety. *Nat Rev Neurosci*. 2004;5:545-552.
6. Gozal EA, O'Neill BE, Sawchuk MA, *et al*. Anatomical and functional evidence for trace amines as unique modulators of locomotor function in the mammalian spinal cord. *Front Neural Circuits*. 2014;8:134.
7. Zimmerman AL, Sawchuk M, Hochman S. Monoaminergic modulation of spinal viscero-sympathetic function in the neonatal mouse thoracic spinal cord. *PLoS One*. 2012;7:e47213.
8. Johnson MD, Heckman CJ. Gain control mechanisms in spinal motoneurons. *Front Neural Circuits*. 2014;8:81.
9. Myers RD. Serotonin and thermoregulation: Old and new views. *J Physiol (Paris)*. 1981;77:505-513.
10. Daubert EA, Condron BG. Serotonin: A regulator of neuronal morphology and circuitry. *Trends Neurosci*. 2010;33:424-434.
11. Harris-Warrick RM, Marder E. Modulation of neural networks for behavior. *Annu Rev Neurosci*. 1991;14:39-57.
12. Lillvis JL, Katz PS. Parallel evolution of serotonergic neuromodulation underlies independent evolution of rhythmic motor behavior. *J Neurosci*. 2013;33:2709-2717.
13. Gaspar P, Cases O, Maroteaux L. The developmental role of serotonin: News from mouse molecular genetics. *Nat Rev Neurosci*. 2003;4:1002-1012.
14. Gross C, Zhuang X, Stark K, *et al*. Serotonin1A receptor acts during development to establish normal anxiety-like behaviour in the adult. *Nature*. 2002;416:396-400.
15. Kawashima T. The role of the serotonergic system in motor control. *Neurosci Res*. 2018;129:32-39.
16. Clarac F, Brocard F, Vinay L. The maturation of locomotor networks. *Prog Brain Res*. 2004;143:57-66.
17. Hultborn H, Nielsen JB. Spinal control of locomotion--from cat to man. *Acta Physiol (Oxf)*. 2007;189:111-121.
18. Leiras R, Cregg JM, Kiehn O. Brainstem circuits for locomotion. *Annu Rev Neurosci*. 2022; 45:63-85.
19. Shik ML, Severin FV, Orlovskiĭ GN. [Control of walking and running by means of electric stimulation of the midbrain]. *Biofizika*. 1966;11:659-666.
20. Brownstone RM, Chopek JW. Reticulospinal systems for tuning motor commands. *Front Neural Circuits*. 2018;12:30.
21. Jordan LM, Liu J, Hedlund PB, Akay T, Pearson KG. Descending command systems for the initiation of locomotion in mammals. *Brain Res Rev*. 2008;57:183-191.
22. Cazalets JR, Sqalli-Houssaini Y, Clarac F. Activation of the central pattern generators for locomotion by serotonin and excitatory amino acids in neonatal rat. *J Physiol*. 1992;455:187-204.
23. Dunbar MJ, Tran MA, Whelan PJ. Endogenous extracellular serotonin modulates the spinal locomotor network of the neonatal mouse. *J Physiol*. 2010;588(Pt 1):139-156.
24. Schmidt BJ, Jordan LM. The role of serotonin in reflex modulation and locomotor rhythm production in the mammalian spinal cord. *Brain Res Bull*. 2000;53:689-710.
25. Liu J, Jordan LM. Stimulation of the parapyramidal region of the neonatal rat brain stem produces locomotor-like activity involving spinal 5-HT7 and 5-HT2A receptors. *J Neurophysiol*. 2005;94:1392-1404.
26. Liu J, Akay T, Hedlund PB, Pearson KG, Jordan LM. Spinal 5-HT7 receptors are critical for alternating activity during locomotion: In vitro neonatal and in vivo adult studies using 5-HT7 receptor knockout mice. *J Neurophysiol*. 2009;102:337-348.
27. Hendricks T, Francis N, Fyodorov D, Deneris ES. The ETS domain factor Pet-1 is an early and precise marker of central serotonin neurons and interacts with a conserved element in serotonergic genes. *J Neurosci*. 1999;19:10348-10356.
28. Hendricks TJ, Fyodorov DV, Wegman LJ, *et al*. Pet-1 ETS gene plays a critical role in 5-HT neuron development and is required for normal anxiety-like and aggressive behavior. *Neuron*. 2003;37:233-247.
29. Nardone R, Höller Y, Thomschewski A, *et al*. Serotonergic transmission after spinal cord injury. *J Neural Transm (Vienna)*. 2015;122:279-295.
30. El Oussini H, Scekic-Zahirovic J, Vercruysse P, *et al*. Degeneration of serotonin neurons triggers spasticity in amyotrophic lateral sclerosis. *Ann Neurol*. 2017;82:444-456.
31. Matjačić Z, Olenšek A, Krajnik J, Eymard B, Zupan A, Pražnikar A. Compensatory mechanisms during walking in response to muscle weakness in spinal muscular atrophy, type III. *Gait Posture*. 2008;27:661-668.
32. Armand S, Mercier M, Watelain E, Patte K, Pelissier J, Rivier F. A comparison of gait in spinal muscular atrophy, type II and Duchenne muscular dystrophy. *Gait Posture*. 2005;21:369-378.

33. Dunaway S, Montes J, Garber CE, *et al*. Performance of the timed "up & go" test in spinal muscular atrophy. *Muscle Nerve*. 2014;50:273-277.
34. Lefebvre S, Bürglen L, Reboullet S, *et al*. Identification and characterization of a spinal muscular atrophy-determining gene. *Cell*. 1995;80:155-165.
35. Wirth B. Spinal muscular atrophy: In the challenge lies a solution. *Trends Neurosci*. 2021;44:306-322.
36. Tisdale S, Pellizzoni L. Disease mechanisms and therapeutic approaches in spinal muscular atrophy. *J Neurosci*. 2015;35:8691-8700.
37. Montes J, Gordon AM, Pandya S, De Vivo DC, Kaufmann P. Clinical outcome measures in spinal muscular atrophy. *J Child Neurol*. 2009;24:968-978.
38. Mentis GZ, Blivis D, Liu W, *et al*. Early functional impairment of sensory-motor connectivity in a mouse model of spinal muscular atrophy. *Neuron*. 2011;69:453-467.
39. Fletcher EV, Simon CM, Pagiazitis JG, *et al*. Reduced sensory synaptic excitation impairs motor neuron function via Kv2.1 in spinal muscular atrophy. *Nat Neurosci*. 2017;20:905-916.
40. Renault F, Raimbault J, Praud J, Laget P. [Electromyographic study of 50 cases of Werdnig-Hoffmann disease]. *Rev Electroencephalogr Neurophysiol Clin*. 1983;13:301-305.
41. Oskoui M, Kim DH, Mentis GZ, De Vivo DC. Transient hyperreflexia: An early diagnostic clue in later-onset spinal muscular atrophy. *Neurol Clin Pract*. 2020;10:e66-e67.
42. Vukojicic A, Delestrée N, Fletcher EV, *et al*. The classical complement pathway mediates microglia-dependent remodeling of spinal motor circuits during development and in SMA. *Cell Rep*. 2019;29:3087-3100.e7.
43. Osman EY, Van Alstyne M, Yen PF, *et al*. Minor snRNA gene delivery improves the loss of proprioceptive synapses on SMA motor neurons. *JCI Insight*. 2020;5:e130574.
44. Simon CM, Van Alstyne M, Lotti F, *et al*. Stasimon contributes to the loss of sensory synapses and motor neuron death in a mouse model of spinal muscular atrophy. *Cell Rep*. 2019;29:3885-3901.e5.
45. Shorrock HK, van der Hoorn D, Boyd PJ, *et al*. UBA1/GARS-dependent pathways drive sensory-motor connectivity defects in spinal muscular atrophy. *Brain*. 2018;141:2878-2894.
46. Ling KK, Lin MY, Zingg B, Feng Z, Ko CP. Synaptic defects in the spinal and neuromuscular circuitry in a mouse model of spinal muscular atrophy. *PLoS One*. 2010;5:e15457.
47. Cerveró C, Blasco A, Tarabal O, *et al*. Glial activation and central synapse loss, but not motoneuron degeneration, are prevented by the sigma-1 receptor agonist PRE-084 in the Smn2B/- mouse model of spinal muscular atrophy. *J Neuropathol Exp Neurol*. 2018;77:577-597.
48. Shorrock HK, Gillingwater TH, Groen EJN. Molecular mechanisms underlying sensory-motor circuit dysfunction in SMA. *Front Mol Neurosci*. 2019;12:59.
49. Buettner JM, Sime Longang JK, Gerstner F, *et al*. Central synaptopathy is the most conserved feature of motor circuit pathology across spinal muscular atrophy mouse models. *iScience*. 2021;24:103376.
50. Simon CM, Janas AM, Lotti F, *et al*. A stem cell model of the motor circuit uncouples motor neuron death from hyperexcitability induced by SMN deficiency. *Cell Rep*. 2016;16:1416-1430.
51. Zagoraiou L, Akay T, Martin JF, *et al*. A cluster of cholinergic premotor interneurons modulates mouse locomotor activity. *Neuron*. 2009;64:645-662.
52. Le TT, Pham LT, Butchbach MER, *et al*. SMNδ7, the major product of the centromeric survival motor neuron (SMN2) gene, extends survival in mice with spinal muscular atrophy and associates with full-length SMN. *Hum Mol Genet*. 2005;14:845-857.
53. Lutz CM, Kariya S, Patruni S, *et al*. Postsymptomatic restoration of SMN rescues the disease phenotype in a mouse model of severe spinal muscular atrophy. *J Clin Invest*. 2011;121:3029-3041.
54. Tanaka H, Amamiya S, Miura N, Araki A, Ohinata J, Fujieda K. Postnatal development of brainstem serotonin-containing neurons projecting to lumbar spinal cord in rats. *Brain Dev*. 2006;28:586-591.
55. Shneider NA, Mentis GZ, Schustak J, O'Donovan MJ. Functionally reduced sensorimotor connections form with normal specificity despite abnormal muscle spindle development: The role of spindle-derived neurotrophin 3. *J Neurosci*. 2009;29:4719-4735.
56. Martinez TL, Kong L, Wang X, *et al*. Survival motor neuron protein in motor neurons determines synaptic integrity in spinal muscular atrophy. *J Neurosci*. 2012;32:8703-8715.
57. Basura GJ, Zhou SY, Walker PD, Goshgarian HG. Distribution of serotonin 2A and 2C receptor mRNA expression in the cervical ventral horn and phrenic motoneurons following spinal cord hemisection. *Exp Neurol*. 2001;169:255-263.
58. Kong XY, Wienecke J, Chen M, Hultborn H, Zhang M. The time course of serotonin 2A receptor expression after spinal transection of rats: An immunohistochemical study. *Neuroscience*. 2011;177:114-126.
59. Vergé D, Calas A. Serotoninergic neurons and serotonin receptors: Gains from cytochemical approaches. *J Chem Neuroanat*. 2000;18(1–2):41-56.
60. Doly S, Madeira A, Fischer J, *et al*. The 5-HT2A receptor is widely distributed in the rat spinal cord and mainly localized at the plasma membrane of postsynaptic neurons. *J Comp Neurol*. 2004;472:496-511.
61. Fonseca MI, Ni YG, Dunning DD, Miledi R. Distribution of serotonin 2A, 2C and 3 receptor mRNA in spinal cord and medulla oblongata. *Brain Res Mol Brain Res*. 2001;89:11-19.
62. Millan MJ. Descending control of pain. *Prog Neurobiol*. 2002;66:355-474.
63. Wallis DI, Wu J, Wang X. Descending inhibition in the neonate rat spinal cord is mediated by 5-hydroxytryptamine. *Neuropharmacology*. 1993;32:73-83.
64. Ziskind-Conhaim L, Seebach BS, Gao BX. Changes in serotonin-induced potentials during spinal cord development. *J Neurophysiol*. 1993;69:1338-1349.
65. García-Ramírez DL, Calvo JR, Hochman S, Quevedo JN. Serotonin, dopamine and noradrenaline adjust actions of myelinated afferents via modulation of presynaptic inhibition in the mouse spinal cord. *PLoS One*. 2014;9:e89999.
66. Honda M, Imaida K, Tanabe M, Ono H. Endogenously released 5-hydroxytryptamine depresses the spinal monosynaptic reflex via 5-HT1D receptors. *Eur J Pharmacol*. 2004;503:55-61.
67. Mentis GZ, Alvarez FJ, Shneider NA, Siembab VC, O'Donovan MJ. Mechanisms regulating the specificity and strength of muscle afferent inputs in the spinal cord. *Ann N Y Acad Sci*. 2010;1198:220-230.
68. Scott MM, Wylie CJ, Lerch JK, *et al*. A genetic approach to access serotonin neurons for in vivo and in vitro studies. *Proc Natl Acad Sci U S A*. 2005;102:16472-7.
69. Kong L, Valdivia DO, Simon CM, *et al*. Impaired prenatal motor axon development necessitates early therapeutic intervention in severe SMA. *Sci Transl Med*. 2021;13:eabb6871.
70. Taylor AS, Glascock JJ, Rose FF, Lutz C, Lorson CL. Restoration of SMN to Emx-1 expressing cortical neurons is not sufficient to provide benefit to a severe mouse model of spinal muscular atrophy. *Transgenic Res*. 2013;22:1029-1036.
71. Liu Q, Dreyfuss G. A novel nuclear structure containing the survival of motor neurons protein. *EMBO J*. 1996;15:3555-3565.

72. Shneider NA, Brown MN, Smith CA, Pickel J, Alvarez FJ. Gamma motor neurons express distinct genetic markers at birth and require muscle spindle-derived GDNF for postnatal survival. *Neural Dev*. 2009;4:42.
73. Simon CM, Dai Y, Van Alstyne M, *et al*. Converging mechanisms of p53 activation drive motor neuron degeneration in spinal muscular atrophy. *Cell Rep*. 2017;21:3767-3780.
74. Van Alstyne M, Simon CM, Sardi SP, Shihabuddin LS, Mentis GZ, Pellizzoni L. Dysregulation of Mdm2 and Mdm4 alternative splicing underlies motor neuron death in spinal muscular atrophy. *Genes Dev*. 2018;32:1045-1059.
75. Rotterman TM, Nardelli P, Cope TC, Alvarez FJ. Normal distribution of VGLUT1 synapses on spinal motoneuron dendrites and their reorganization after nerve injury. *J Neurosci*. 2014;34:3475-3492.
76. Jordan LM, Sławińska U. Chapter 12--modulation of rhythmic movement: Control of coordination. *Prog Brain Res*. 2011;188:181-195.
77. Cabaj AM, Majczyński H, Couto E, *et al*. Serotonin controls initiation of locomotion and afferent modulation of coordination via 5-HT(7) receptors in adult rats. *J Physiol*. 2017;595:301-320.
78. Marlier L, Teilhac JR, Cerruti C, Privat A. Autoradiographic mapping of 5-HT1, 5–HT1A, 5-HT1B and 5-HT2 receptors in the rat spinal cord. *Brain Res*. 1991;550:15-23.
79. Perrier JF, Rasmussen H, Christensen R, Petersen A. Modulation of the intrinsic properties of motoneurons by serotonin. *Curr Pharm Des*. 2013;19:4371-4384.
80. Alvarez FJ, Pearson JC, Harrington D, Dewey D, Torbeck L, Fyffe REW. Distribution of 5-hydroxytryptamine-immunoreactive boutons on alpha-motoneurons in the lumbar spinal cord of adult cats. *J Comp Neurol*. 1998;393:69-83.
81. Wang MY, Dun NJ. 5-Hydroxytryptamine Responses in neonate rat motoneurones in vitro. *J Physiol*. 1990;430:87-103.
82. Cotel F, Exley R, Cragg SJ, Perrier JF. Serotonin spillover onto the axon initial segment of motoneurons induces central fatigue by inhibiting action potential initiation. *Proc Natl Acad Sci U S A*. 2013;110:4774-4779.
83. Crick H, Wallis DI. Inhibition of reflex responses of neonate rat lumbar spinal cord by 5-hydroxytryptamine. *Br J Pharmacol*. 1991;103:1769-1775.
84. Machacek DW, Garraway SM, Shay BL, Hochman S. Serotonin 5-HT(2) receptor activation induces a long-lasting amplification of spinal reflex actions in the rat. *J Physiol*. 2001;537(Pt 1):201-207.
85. Ladewig T, Lalley PM, Keller BU. Serotonergic modulation of intracellular calcium dynamics in neonatal hypoglossal motoneurons from mouse. *Brain Res*. 2004;1001:1-12.
86. Singer JH, Bellingham MC, Berger AJ. Presynaptic inhibition of glutamatergic synaptic transmission to rat motoneurons by serotonin. *J Neurophysiol*. 1996;76:799-807.
87. Daval G, Vergé D, Basbaum AI, Bourgoin S, Hamon M. Autoradiographic evidence of serotonin1 binding sites on primary afferent fibres in the dorsal horn of the rat spinal cord. *Neurosci Lett*. 1987;83:71-76.
88. Yomono HS, Suzuki H, Yoshioka K. Serotonergic fibers induce a long-lasting inhibition of monosynaptic reflex in the neonatal rat spinal cord. *Neuroscience*. 1992;47:521-531.
89. Zhang H, Robinson N, Wu C, Wang W, Harrington MA. Electrophysiological properties of motor neurons in a mouse model of severe spinal muscular atrophy: In vitro versus in vivo development. *PLoS One*. 2010;5:e11696.
90. Molliver ME. Serotonergic neuronal systems: What their anatomic organization tells us about function. *J Clin Psychopharmacol*. 1987;7(6 Suppl):3S-23S.
91. Hornung JP. The human raphe nuclei and the serotonergic system. *J Chem Neuroanat*. 2003;26:331-343.
92. Steinbusch HW. Distribution of serotonin-immunoreactivity in the central nervous system of the rat-cell bodies and terminals. *Neuroscience*. 1981;6:557-618.
93. Kurosawa Y, Aoki M. [Distribution pattern of lumbar epaxial, especially M. multifidus motoneurons in the spinal cord of the cat: A study by the retrograde horseradish peroxidase method]. *Hokkaido Igaku Zasshi*. 1987;62:145-156.
94. Wadman RI, Wijngaarde CA, Stam M, *et al*. Muscle strength and motor function throughout life in a cross-sectional cohort of 180 patients with spinal muscular atrophy types 1c-4. *Eur J Neurol*. 2018;25:512-518.
95. D'Amico A, Mercuri E, Tiziano FD, Bertini E. Spinal muscular atrophy. *Orphanet J Rare Dis*. 2011;6:71.
96. Sucato DJ. Spine deformity in spinal muscular atrophy. *J Bone Joint Surg Am*. 2007;89(Suppl 1):148-154.
97. Merlini L, Granata C, Bonfiglioli S, Marini ML, Cervellati S, Savini R. Scoliosis in spinal muscular atrophy: Natural history and management. *Dev Med Child Neurol*. 1989;31:501-508.
98. Bayliss DA, Umemiya M, Berger AJ. Inhibition of N- and P-type calcium currents and the after-hyperpolarization in rat motoneurones by serotonin. *J Physiol*. 1995;485(Pt 3):635-647.
99. Perrier JF, Alaburda A, Hounsgaard J. 5-HT1A Receptors increase excitability of spinal motoneurons by inhibiting a TASK-1-like K+ current in the adult turtle. *J Physiol*. 2003;548(Pt 2):485-492.
100. Talley EM, Sadr NN, Bayliss DA. Postnatal development of serotonergic innervation, 5–HT1A receptor expression, and 5-HT responses in rat motoneurons. *J Neurosci*. 1997;17:4473-4485.
101. Bubar MJ, Seitz PK, Thomas ML, Cunningham KA. Validation of a selective serotonin 5-HT(2C) receptor antibody for utilization in fluorescence immunohistochemistry studies. *Brain Res*. 2005;1063:105-113.
102. Hounsgaard J, Hultborn H, Jespersen B, Kiehn O. Bistability of alpha-motoneurones in the decerebrate cat and in the acute spinal cat after intravenous 5-hydroxytryptophan. *J Physiol*. 1988;405:345-367.
103. Dunaway Young S, Montes J, Salazar R, *et al*. Scoliosis surgery significantly impacts motor abilities in higher-functioning individuals with spinal muscular atrophy1. *J Neuromuscul Dis*. 2020;7:183-192.
104. Bos R, Sadlaoud K, Boulenguez P, *et al*. Activation of 5-HT2A receptors upregulates the function of the neuronal K-Cl cotransporter KCC2. *Proc Natl Acad Sci U S A*. 2013;110:348-353.
105. Thirumalai V, Behrend RM, Birineni S, Liu W, Blivis D, O'Donovan MJ. Preservation of VGLUT1 synapses on ventral calbindin-immunoreactive interneurons and normal locomotor function in a mouse model of spinal muscular atrophy. *J Neurophysiol*. 2013;109:702-710.
106. Strain MM, Kauer SD, Kao T, Brumley MR. Inter- and intralimb adaptations to a sensory perturbation during activation of the serotonin system after a low spinal cord transection in neonatal rats. *Front Neural Circuits*. 2014;8:80.
107. Myoga H, Nonaka S, Matsuyama K, Mori S. Postnatal development of locomotor movements in normal and para-chlorophenylalanine-treated newborn rats. *Neurosci Res*. 1995;21:211-221.
108. Pflieger JF, Clarac F, Vinay L. Postural modifications and neuronal excitability changes induced by a short-term serotonin depletion during neonatal development in the rat. *J Neurosci*. 2002;22:5108-5117.

109. Montes J, McDermott MP, Martens WB, *et al*. Six-minute walk test demonstrates motor fatigue in spinal muscular atrophy. *Neurology*. 2010;74:833-838.
110. Montes J, McDermott MP, Mirek E, *et al*. Ambulatory function in spinal muscular atrophy: Age-related patterns of progression. *PLoS One*. 2018;13:e0199657.
111. Allam AM, Schwabe AL. Neuromuscular scoliosis. *PM R*. 2013;5: 957-963.
112. Yao M, Xia Y, Feng Y, *et al*. Anxiety and depression in school-age patients with spinal muscular atrophy: A cross-sectional study. *Orphanet J Rare Dis*. 2021; 16:385.